

# SUPERDARN SCALAR RADAR EQUATIONS

O.I. BERNGARDT, K.A. KUTELEV, A.P. POTEKHIN

**ABSTRACT.** The quadratic scalar radar equations are obtained for SuperDARN radars that are suitable for the analysis and interpretation of experimental data. The paper is based on a unified approach to the obtaining radar equations for the monostatic and bistatic sounding with use of hamiltonian optics and ray representation of scalar Green's function and without taking into account the polarization effects. The radar equation obtained is the sum of several terms corresponding to the propagation and scattering over the different kinds of trajectories, depending on their smoothness and the possibility of reflection from the ionosphere. It is shown that the monostatic sounding in the media with significant refraction, unlike the case of refraction-free media, should be analyzed as a combination of monostatic and bistatic scattering. This leads to strong dependence of scattering amplitude on background ionospheric density due to focusing mechanism and appearance of new (bistatic) areas of effective scattering with significant distortion of the scattered signal spectrum. Selective properties of the scattering also have been demonstrated.

## 1. INTRODUCTION

Investigations of ionosphere and magnetosphere with use of international network of SuperDARN(Super Dual Auroral Radar Network) radars becomes one of the basic techniques for analysis of the processes in the high-latitude ionosphere and magnetosphere today [Ruohoniemi et al.(1988), Ruohoniemi et al.(1989), Greenwald et al.(1995), Chisham et al.(2007), Ruohoniemi et al.(2011)]. Expanding of the network to the mid-latitudes allows to investigate expanding the polar effects to the mid-latitudes during geomagnetic disturbances and storms[Baker et al.(2007)]. In spite of wide use of the data the inversion technique for this method - obtaining the parameters of the ionosphere from the received signals is still under development. Today taking into account the ionospheric refraction to the scattered signal characteristics is important theoretical problem [Nasyrov(1991), Uspensky et al.(1994a), Uspensky et al.(1994b), Ponomarenko et al.(2009), Gillies et al.(2009), Ponomarenko et al.(2010), Gillies et al.(2011), Spaleta et al.(2015)].

The basis for the backscattering technique, used by the SuperDARN radars is the radar equation. It relates the shape of the correlation function of the received signal with spectral density of irregularities and characteristics of background ionosphere.

Currently the SuperDARN radar equation exists only in very simple approximations [Schiffler(1996)], which can lead to potential problems in data interpretation. For example, correct taking into account the refraction in the evaluation of the basic SuperDARN parameter - irregularities velocity [Gillies et al.(2011)].

Traditionally, to interpret the SuperDARN measurements there is used an analogy [Schiffler(1996)] with the radar equation in refraction-free case [Tatarsky(1967), Ishimaru(1978)]. Initially, this radar equation was developed for the case of scatterers that are small compared with the Fresnel zone radius, and not always valid for irregularities with the size compared with this radius. In [Berngardt and Potekhin(2000), Berngardt and Potekhin(2002)] there was obtained the radar equation under assumption of smooth spatial changes of spectral density of irregularities. This refraction-free radar equation is valid for scattering by large-scale ionospheric irregularities including irregularities elongated with the Earth magnetic field and studied by SuperDARN radars. But correct taking into account the refraction was not done yet.

In the paper we obtained the scalar radar equation for SuperDARN radars within the first propagation hop, taking into account refraction and single reflection from the ionosphere.

## 2. INITIAL EQUATIONS

**2.1. Ray representation of Green's function.** Traditionally the problems of radiowave propagation and scattering in smoothly inhomogeneous media are analyzed using Green's function approach. Radiowave propagation in smoothly inhomogeneous media can be described using geometrical optics (WKB approximation)[Heading(1962), Kravtsov and Orlov(1990)]. Geometroptical approach allows to replace extended source (antenna) by point source and distribution of the transmitted signal over the ray exit directions (antenna pattern). The full geometroptical Green's function is matrix-valued (see, for example [Kravtsov et al.(1996), Liang and Wan(1997)]):

$$(1) \quad \begin{aligned} \vec{E}(\vec{r}, \omega) &= \hat{G}(\vec{R}_0, \vec{r}, \omega) \vec{a}(\omega) \\ \hat{G}(\vec{R}_0, \vec{r}, \omega) &= \frac{1}{F^{1/2}(\vec{R}_0, \vec{r})} e^{i\frac{\omega}{c}\psi(\vec{R}_0, \vec{r})} \hat{\Gamma}(\vec{R}_0, \vec{r}) \end{aligned}$$

where  $\hat{\Gamma}(\vec{R}_0, \vec{r})$  - polarization matrix,  $F^{1/2}(\vec{R}_0, \vec{r})$  - decrease of the signal with the range,  $\psi(\vec{R}_0, \vec{r})$  - geometroptical eikonal;  $\vec{R}_0$  is the position of the transmitter.

The problem of the formula is impossibility to use it in the tasks of multipath propagation, when signal has a number of different trajectories to reach the same scattering point[Kravtsov and Namazov(1980)]. To generalize (1) for the problem of multipath propagation lets use the ray coordinate system and analyze the field in a given point as a result of interference of several geometroptical rays with different exit

angles. In simpler scalar case (which does not take into account the polarization of the electromagnetic wave) we can make the equivalent ray representation for scalar Green's function  $G_{go}(\vec{R}_0, \vec{\Lambda}, \omega)$ , that after integrating over the ray coordinates results into standard scalar Green's function:

$$(2) \quad G(\vec{R}_0, \vec{r}', \omega) = \int G_{go}(\vec{R}_0, \vec{\Lambda}, \omega) \delta(\vec{r}' - \vec{R}(\vec{\Lambda})) F(\vec{\Lambda}) d\vec{\Lambda}$$

Here  $G_{go}(\vec{R}_0, \vec{\Lambda}, \omega)$  is Green's function ray representation as a function of ray arguments  $\vec{\Lambda}$ , antenna position  $\vec{R}_0$  and frequency of the signal  $\omega$ ;  $\vec{R}(\vec{\Lambda})$  is ray trajectory for given ray coordinates  $\vec{\Lambda}$ ;

$$(3) \quad F(\vec{\Lambda}) = \left\| \frac{\partial R_i(\vec{\Lambda})}{\partial \Lambda_j} \right\|$$

is Jacobian to convert from ray coordinates to spatial coordinates (and at the same time the square of geometrical divergence);  $\vec{\Lambda} = (\hat{\Lambda}; \Lambda_{\parallel}) = (\hat{\Lambda}_{\xi}, \hat{\Lambda}_{\eta}; S)$  are the ray coordinates - two ray exit angles and trajectory group length;  $d\vec{\Lambda} = d\Lambda_{\parallel} d\hat{\Lambda}_{\xi} d\hat{\Lambda}_{\eta}$ .

After taking into account antenna pattern  $g(\hat{\Lambda}, \omega)$  of the transmitter, the signal in the position of the scatterer  $\vec{r}$  can be calculated (with accuracy of constant multiplier) from the integral representation (2), as a superposition of the fields, propagating over the different trajectories:

$$(4) \quad u(\vec{r}, \omega) = \int a(\omega) g(\hat{\Lambda}, \omega) G_{go}(\vec{R}_0, \vec{\Lambda}, \omega) \delta(\vec{r} - \vec{R}(\vec{\Lambda})) F(\vec{\Lambda}) d\vec{\Lambda}$$

where

$$(5) \quad G_{go}(\vec{R}_0, \vec{\Lambda}, \omega) = \frac{1}{F^{1/2}(\vec{\Lambda})} e^{i\frac{\omega}{c}\psi(\vec{\Lambda}, \omega)}$$

$\psi(\vec{\Lambda}, \omega)$  is eikonal in ray coordinates;  $\vec{R}(\vec{\Lambda})$  is ray trajectory;  $a(\omega)$  - transmitted signal spectrum for frequency  $\omega$ .

The given representation (4) has the simple physical sense: the signal that comes to the point  $\vec{r}$  is a superposition of geometrooptical rays, transmitted from the antenna with different ray directions  $\hat{\Lambda}$  and amplitudes  $g$ . The correspondence of the representation (4) to the traditional geometrooptical representation for the signal can be shown by integrating (4) over the  $d\vec{\Lambda}$  and taking into account that integrating of delta-function under integral produces the transformation Jakobian (3) and summation over all propagation trajectories  $\nu$  to the given point  $\vec{r}$ :

$$(6) \quad \int g(\vec{\Lambda}) \delta(\vec{r}' - \vec{R}(\vec{\Lambda})) d\vec{\Lambda} = \sum_{\nu} \left\| \frac{\partial}{\partial \Lambda_j} R_i(\vec{\Lambda}) \right\|_{\nu}^{-1} g(\vec{R}^{-1}(\vec{r}'))$$

After integration the signal (4) transforms into:

$$(7) \quad \begin{cases} u(\vec{r}', \omega) = \sum_{\nu} \frac{a(\omega) g(\vec{\Lambda}_{\nu}, \omega)}{F^{1/2}(\vec{\Lambda}_{\nu})} e^{i \frac{\omega}{c} \psi(\vec{R}(\vec{\Lambda}_{\nu}))} \\ \vec{r}' = \vec{R}(\vec{\Lambda}_{\nu}) \end{cases}$$

The trajectories  $\nu$  are defined by second equation of the system (7) for any given  $\vec{r}'$ . This equation is close to discussed in [Kravtsov and Namazov(1980)].

**2.2. Ray equations: Hamilton representation.** The eikonal  $\psi(\vec{\Lambda})$  is defined as the integral over the curvilinear trajectory, definable as a propagation in background ionosphere of the ray with given exit angle  $\hat{\Lambda}$ . The trajectory shape depends on the refractivity index distribution  $n(\vec{R}(\hat{\Lambda}, \sigma))$  in the ionosphere. Traditionally, the calculations of rays for the decameter propagation are made in hamiltonian optics approach [Kravtsov and Orlov(1990)]. In this approach, the ray trajectory is defined as a solution of the Hamilton equations, and depends on the ray coordinates chosen. The choice of ray coordinates depends on the convenience and on the structure of Hamiltonian.

The eikonal  $\psi$  in the equations (1,5,7) is also calculated from the Hamiltonian  $H(\vec{P}, \vec{R})$ , generalized momentum  $\vec{P}$  and generalized coordinate  $\vec{R}$ . One of the most used Hamiltonian  $H(\vec{P}, \vec{R})$  in geometrical optics is [Kravtsov and Orlov(1990)]:

$$(8) \quad H(\vec{P}, \vec{R}) = \frac{1}{2} \left\{ P^2 - n^2(\vec{R}) \right\} = 0$$

In this case the Hamilton equations, that allows to calculate the ray trajectory and eikonal are:

$$(9) \quad \begin{cases} P = n(\vec{R}) \\ \frac{\partial \vec{R}}{\partial S} = \vec{P} \\ \frac{\partial \vec{P}}{\partial S} = n \vec{\nabla} n(\vec{R}) \\ \vec{\nabla} \psi = \vec{P} \end{cases}$$

In this representation (8)  $S = \Lambda_{\parallel}$  is ray coordinate, that is equivalent to the trajectory group length. Eikonal, generalized coordinate and momentum are obtained by integrating (9) over the ray trajectory:

$$(10) \quad \left\{ \begin{array}{l} \vec{R} = \vec{R}_0 + \int_{S_0}^S \vec{P} dS' \\ \vec{P} = \vec{P}_0 + \int_{S_0}^S n \vec{\nabla} n(\vec{R}(S')) dS' \\ \psi = \psi_0 + \int_{S_0}^S P^2 dS' \end{array} \right.$$

The hamiltonian optics representation is useful for numerical calculations and is widely used in the problems of radiowave propagation (as characteristics method)[Kravtsov and Orlov(1990), Settimi et al.(2014)], including SuperDARN problems [Gauld et al.(2002), Ponomarenko et al.(2009), Ponomarenko et al.(2010), Ponomarenko et al.(2011), Berngardt et al.(2015a)].

**2.3. Initial representation of the scattered signal.** One can see that ray representation of Green's function (5) is the product of fast and slow oscillating functions. Spatial multiplier  $g(\hat{\Lambda}, \omega)$  is a smooth function of the frequency, transmitted signal  $a(\omega)$  is narrowband near carrier frequency  $\omega_0$ . In this case we can represent fast oscillating phase  $\frac{\omega}{c}\psi(\vec{\Lambda}, \omega)$  as a Taylor series near  $\omega_0$ , with the small parameter  $|\omega - \omega_0| \ll \omega_0$  and get the temporal representation of the propagating signal:

$$(11) \quad \begin{aligned} u(\vec{r}, t) &\approx e^{i\omega_0 t} U(\vec{r}, t) \\ U(\vec{r}, t) &\approx \int A(t - T_r) g(\hat{\Lambda}, \omega_0) F^{1/2}(\vec{\Lambda}, \omega_0) e^{ik_0 \psi(\vec{\Lambda}, \omega_0)} \delta(\vec{r} - \vec{R}(\vec{\Lambda}, \omega_0)) d\vec{\Lambda} \end{aligned}$$

Here  $k_0 = \frac{\omega_0}{c}$  is wavenumber of transmitted signal;  $U(\vec{r}, t)$  is the complex envelope of propagating signal;  $A(t - T_r)$  is complex envelope of the sounding signal;

$$(12) \quad T_{r,t} = \frac{\partial}{\partial \omega} \left( \frac{\omega}{c} \psi(\vec{\Lambda}, \omega) \right)_{\omega=\omega_0}$$

is the group delay of the propagating signal.

Necessary condition of narrowband signal (with spectral width  $\Delta\omega$ ) is defined as smallness of second differential of fast oscillating phase in temporal representation of (5):

$$(13) \quad (\Delta\omega)^2 \frac{\partial^2}{\partial \omega^2} \left( \frac{\omega}{c} \psi(\vec{\Lambda}, \omega) \right)_{\omega=\omega_0} \ll 1$$

So, the obtained equation (11) is valid in the regions, where antenna pattern, refractivity index and geometroptical divergence are changing slowly over the band  $\Delta\omega$  of the sounding signal  $a(\omega)$ .

In Fig.1 are shown the validity (13) regions calculated for reference ionosphere model, typical SuperDARN frequency (10MHz) and typical radar pulse durations (100 and 300usec.). The signal trajectories were calculated by the method of characteristics for cold isotropic plasma given by IRI-2012 model [Bilitza et al.(2011)]. As one can see from Fig.1, the approximation of the narrowband signal (13) is valid almost everywhere, except for a small number of rays near the Pedersen ray after reflection point. For longer pulses (300usec), this area is smaller than for shorter ones (100usec). Qualitatively, this can be explained as follows: near the Pedersen ray small changes of signal frequency will lead to a big changes of the trajectory (high frequency components of the signal propagates upward, and the low frequency components propagates downward). Thus, when propagating over these trajectories the signal envelope in the ionosphere is not the same as the transmitted signal envelope, and one should whether do not consider any of these areas, or take into account the signal distortions at these trajectories correctly.

Below in the paper we consider only the trajectories at which the narrowband condition (13) is valid, and use in (11) the equality sign.

By the same way we can obtain the expression for the scattered signal at the receiving antenna:

$$(14) \quad U(t) \approx k_0^2 \int \varepsilon(\vec{r}, t - T_t) A(t - T_r - T_t) D(\vec{\Lambda}_r, \vec{\Lambda}_t, \omega_0) e^{ik_0 \Psi(\vec{\Lambda}_r, \vec{\Lambda}_t, \omega_0)} \cdot \delta(\vec{r} - \vec{R}_r(\vec{\Lambda}_r, \omega_0)) \delta(\vec{r} - \vec{R}_t(\vec{\Lambda}_t, \omega_0)) d\vec{\Lambda}_t d\vec{\Lambda}_r d\vec{r}$$

where

$\vec{\Lambda}_r, \vec{\Lambda}_t$  - ray coordinate systems relative to receiver and transmitter correspondingly;

$\psi_r(\vec{\Lambda}_r, \omega_0), \psi_t(\vec{\Lambda}_t, \omega_0)$  are the trajectory phase lengths from the scatterer position  $\vec{R}_r(\vec{\Lambda}_r, \omega_0)$  to the receiver and transmitter correspondingly;

$\Psi(\vec{\Lambda}_r, \vec{\Lambda}_t, \omega_0) = \psi_r(\vec{\Lambda}_r, \omega_0) + \psi_t(\vec{\Lambda}_t, \omega_0)$  is the full trajectory phase length (eikonal);

$$(15) \quad D(\vec{\Lambda}_r, \vec{\Lambda}_t, \omega_0) = g_r^*(\hat{\Lambda}_r, \omega_0) g_t(\hat{\Lambda}_t, \omega_0) F_r^{1/2}(\vec{\Lambda}_r, \omega_0) F_t^{1/2}(\vec{\Lambda}_t, \omega_0)$$

is the spatial multiplier, defined by antenna patterns  $g_r(\hat{\Lambda}_r, \omega_0), g_t(\hat{\Lambda}_t, \omega_0)$  of receiver and transmitter correspondingly, and by geometrical divergence; indexes  $t, r$  mark trajectories of transmitting (trajectory from transmitter to the scatterer) and receiving (trajectory from receiver to scatterer) correspondingly;  $\vec{R}_t(\vec{\Lambda}_t), \vec{R}_r(\vec{\Lambda}_r)$  are the positions of the scatterer as a function of ray coordinates (ray direction and radar range) in transmitter coordinate system and receiver coordinate system correspondingly;  $T_r, T_t$  are group delays (12) from scatterer to transmitter and receiver correspondingly; delta-functions define the condition that scatterer position corresponds

to the coincidence of the ends of trajectories from transmitter and receiver (and at the same time are keeping the ability of several propagation trajectories to the scatterer);  $\varepsilon(\vec{r}, t)$  is dielectric permittivity variations.

Integrating over the  $d\vec{r}$  allows to simplify the expression (14) and represent it as an integral over the ray coordinates of transmitting and receiving rays:

$$(16) \quad U(t) = k_0^2 \int \varepsilon(\vec{R}_t(\vec{\Lambda}_t, \omega_0), t - T_t) A(t - T_r - T_t) D(\vec{\Lambda}_r, \vec{\Lambda}_t, \omega_0) \cdot e^{ik_0\Psi(\vec{\Lambda}_r, \vec{\Lambda}_t, \omega_0)} \delta(\vec{R}_r(\vec{\Lambda}_r, \omega_0) - \vec{R}_t(\vec{\Lambda}_t, \omega_0)) d\vec{\Lambda}_t d\vec{\Lambda}_r$$

Delta-function under the integral in the case of several propagation trajectories to the scatterer will be transformed into the cross-sum over these trajectories after integrating over the  $\vec{\Lambda}_t, \vec{\Lambda}_r$ .

It is important to note that this equation is valid for narrowband sounding and received signals (13) (where  $\Delta\omega$  is the sum of the bands of sounding signal  $a(\omega)$  and dielectric permittivity fluctuations  $\varepsilon(\omega)$ ) and in absence of caustics for given group delay  $t$ .

For obtaining SuperDARN radar equations we will consider this equation in the cases of monostatic and bistatic sounding.

### 3. MONOSTATIC SOUNDING: SINGLE TRAJECTORY CASE

In monostatic case the position of the receiver and the transmitter coincides, so the functions  $\vec{R}_t(\vec{\Lambda}_t), \vec{R}_r(\vec{\Lambda}_r)$  coincide too and can be represented as a same function  $\vec{R}(\vec{\Lambda})$ , but from different ray arguments  $\vec{\Lambda}_t, \vec{\Lambda}_r$ . In this case the expression for the received signal (16) becomes:

$$(17) \quad U(t) = k_0^2 \int \varepsilon(\vec{R}(\vec{\Lambda}_t), t - T_t) A(t - T_r - T_t) D(\vec{\Lambda}_r, \vec{\Lambda}_t, \omega_0) \cdot e^{ik_0\Psi(\vec{\Lambda}_r, \vec{\Lambda}_t)} \delta(\vec{R}(\vec{\Lambda}_r) - \vec{R}(\vec{\Lambda}_t)) d\vec{\Lambda}_t d\vec{\Lambda}_r$$

Here we excluded all the evident arguments of the functions. The expression (17) describes both single and multiple trajectory cases for the case of monostatic sounding.

**3.1. Single trajectory case.** To illustrate the approach of obtaining radar equation let's analyze the simplest case: there is only a single trajectory to reach scatterer from the transmitter. This corresponds to the case when  $\vec{R}(\vec{\Lambda}_r)$  is a bijective function. In this case the integral over the  $d\vec{\Lambda}_r$  in (17) can be calculated. The rest argument  $\vec{\Lambda}_t$  can be renamed to  $\vec{\Lambda}$ , additional multiplier  $F_r^{-1}$  arises due to integration of delta-function, and the expression for the scattered signal (17) becomes:

$$(18) \quad U(t) = \int \varepsilon(\vec{R}(\vec{\Lambda}), t - T(\vec{\Lambda})) A(t - 2T(\vec{\Lambda})) D_u(\vec{\Lambda}, \omega_0) e^{i2k_0\Psi(\vec{\Lambda})} d\vec{\Lambda}$$

where

$$(19) \quad D_u(\vec{\Lambda}_r, \omega_0) = g_r^*(\hat{\Lambda}, \omega_0) g_t(\hat{\Lambda}, \omega_0)$$

Usually, when interpreting SuperDARN data, the average autocorrelation function of the signal [Greenwald et al.(1995), Chisham et al.(2007), Ribeiro et al.(2013)] is analysed:

$$(20) \quad P(t, \Delta T) = \langle U(t)U^*(t + \Delta T) \rangle$$

To get the radar equation, by analogy with [Berngardt and Potekhin(2000), Berngardt and Potekhin(2002)], lets use the following characteristics:

$$(21) \quad \Phi(\vec{r}; \vec{\rho}, \Delta T) = \langle \varepsilon(\vec{r}, t) \varepsilon^*(\vec{r} + \vec{\rho}, t + \Delta T) \rangle$$

is the stationary spatio-temporal correlation function of the irregularities, that defines statistical characteristics of the scatterers;

$$(22) \quad W(t, S, \Delta T, \Delta S) = A(t - S/c)A^*(t - S/c + \Delta T + \Delta S/c)$$

is the weight volume, that defines spatial selection of the irregularities over the radar range (defined by two-way distance  $S$ ) and selection of the irregularities over the correlation function lag (defined by parameter  $\Delta T$ );

$$(23) \quad \begin{aligned} D_\Sigma(\vec{\Lambda}, \vec{\Lambda}_2) &= D_u(\vec{\Lambda}, \omega_0) D_u^*(\vec{\Lambda}_2, \omega_0) = \\ &= g_r^*(\hat{\Lambda}_r, \omega_0) g_t(\hat{\Lambda}_t, \omega_0) g_r^*(\hat{\Lambda}_{r,2}, \omega_0) g_t(\hat{\Lambda}_{t,2}, \omega_0) \end{aligned}$$

is spatial multiplier that defines the contribution of antenna patterns.

The average autocorrelation function of the received signal (20) can be represented as following temporal and spectral radar equations:

$$(24) \quad \begin{aligned} P(t, \Delta T) &= \int \Phi(\vec{R}(\vec{\Lambda}); \vec{R}(\vec{\Lambda}') - \vec{R}(\vec{\Lambda}), \Delta T - T(\vec{\Lambda}') + T(\vec{\Lambda})) \cdot \\ &\cdot W(t, T(\vec{\Lambda})c, \Delta T, \{T(\vec{\Lambda}') - T(\vec{\Lambda})\}c) D_\Sigma(\vec{\Lambda}, \vec{\Lambda}') e^{i2k_0\{\psi(\vec{\Lambda}) - \psi(\vec{\Lambda}')\}} d\vec{\Lambda} d\vec{\Lambda}' \end{aligned}$$

$$(25) \quad \begin{aligned} \tilde{P}(t, \omega) &= \int \tilde{\Phi}(\vec{R}(\vec{\Lambda}); \vec{k}, \nu) \tilde{W}(t, T(\vec{\Lambda})c, \omega - \nu, \{T(\vec{\Lambda}') - T(\vec{\Lambda})\}c) \cdot \\ &\cdot e^{i\nu\{T(\vec{\Lambda}) - T(\vec{\Lambda}')\}} D_\Sigma(\vec{\Lambda}, \vec{\Lambda}') e^{-i\vec{k}(\vec{R}(\vec{\Lambda}) - \vec{R}(\vec{\Lambda}'))} e^{i2k_0(\psi(\vec{\Lambda}) - \psi(\vec{\Lambda}'))} d\vec{\Lambda} d\vec{\Lambda}' d\nu d\vec{k} \end{aligned}$$

Here  $\tilde{A}$  marks Fourier transform of  $A$  over one of its arguments;  $\tilde{\Phi}(\vec{R}(\vec{\Lambda}); \vec{k}, \nu)$  is spectral density of the irregularities.

It is difficult to use these equations for interpreting the experimental data because of the fast oscillating functions under integral. But, some

of the integrands in (24,25) do not depend on  $\vec{\Lambda}'$ , the other can be considered slightly dependent on it. So we can successfully integrate the equations: at first over the  $d\vec{\Lambda}'$ , and than over the  $d\vec{\Lambda}$ .

To obtain a convenient representation of (24,25) we need to integrate fast oscillating functions like:

$$(26) \quad I = \int Z(\vec{\Lambda}) e^{i(-\vec{k} \vec{R}(\vec{\Lambda}, \omega_0) + 2k_0 \psi(\vec{\Lambda}, \omega_0))} d\vec{\Lambda}$$

where  $Z(\vec{\Lambda})$  is a function that is smooth in comparison with fast-oscillating exponent. By analogy with [Berngardt and Potekhin(2000), Berngardt and Potekhin(2002)] lets use a combination of the stationary phase method [Fedoryuk(1989)] and Fourier transform for this.

### 3.2. Integrating fast oscillating functions.

3.2.1. *Convenient ray coordinates.* The initial equations for the scattered signal (25) are given in their basic representation, without specifying the exact ray coordinate system  $\vec{\Lambda}$ . Different ones can be used for this [Kravtsov and Orlov(1990)]. The fast oscillating integrand (26) in hamiltonian representation for case (10) becomes:

$$(27) \quad I = \int Z(\vec{\Lambda}) e^{i \left( \int_0^S \{-\vec{k} \vec{P}(\hat{\Lambda}, S') + 2k_0 P^2(\hat{\Lambda}, S')\} dS' \right)} d\hat{\Lambda}_\xi d\hat{\Lambda}_\eta dS$$

The most convenient technique for the calculation of fast oscillating integrals is the method of stationary phase (MSP)[Fedoryuk(1989)]. In this case, the integral can be expressed as the sum of the contributions of the stationary points (points at which the derivative of fast-changing phase over the integration variable becomes zero), and the contribution is inversely proportional to the square root of second derivative of the fast oscillating phase at this point (characteristic scale). The criterion for the applicability of this method is small changes of the other integrands at the characteristic scale [Fedoryuk(1989)].

To check convenience of the ray coordinate system lets calculate the integral (27) by stationary phase method over the ray exit angles  $\hat{\Lambda} = (\hat{\Lambda}_\xi, \hat{\Lambda}_\eta)$  that is convenient for this problem [Berngardt and Potekhin(2000), Berngardt and Potekhin(2002)].

The detailed calculation by stationary phase method showed, that it is convenient to choose the coordinates system that provides

$$(28) \quad \left\{ \vec{P} \frac{\partial \vec{P}}{\partial \hat{\Lambda}} \right\}_{\Lambda_{||} = const} = 0$$

that is valid for refraction-free or homogeneous background ionosphere. In this case obtaining and interpreting the radar equations will be similar to the approach developed for VHF [Berngardt and Potekhin(2000)]. Due to the generalized momentum  $\vec{P}$  is perpendicular to the wave front at any given moment [Babich and Buldyrev(1978), p.24], we should use instead of the trajectory length coordinate  $\Lambda_{\parallel}$  the trajectory group length  $S$  (or group delay of the signal  $dT = \frac{dL}{cn}$ ), that provides (28). In this case, one can use the system of Hamiltonian equations, described above (9,10) and analyze the integral (27).

Using (9,10) it can be shown that stationary point condition  $\frac{\partial \varphi}{\partial \hat{\Lambda}} = 0$  corresponds to:

$$(29) \quad \left\{ \frac{\partial}{\partial \hat{\Lambda}} \int_0^S (\vec{k} \vec{P}) dS' \right\}_{\hat{\Lambda}=\hat{\Lambda}_{SF}} = \int_0^S \left\{ \vec{k} \left( \frac{\partial \vec{P}}{\partial \hat{\Lambda}} \right)_{\perp \vec{P}} \right\}_{\hat{\Lambda}=\hat{\Lambda}_{SF}} dS' = 0$$

This means that stationary point is the point where the projection of the irregularities wave vector  $\vec{k}$  to the perpendicular to the generalized momentum  $\vec{P}$  'in average' (as an integral along the trajectory) equals to zero. In other words, the irregularities wave vector  $\vec{k}$  is 'in average' should be perpendicular to the wave front.

So the stationary point (29) for coordinate system  $(\hat{\Lambda}, S)$  can be represented as:

$$(30) \quad \int_0^S \vec{k} \vec{P} dS' = - \int_0^S k P dS'$$

For locally-homogeneous trajectory, i.e. for trajectory, at which the refraction coefficient is nearly constant at investigated part of the trajectory ( $P = const$ ), the stationary point can be represented not as the 'average' integral condition (29), but as the local condition:

$$(31) \quad \vec{k} \vec{P} = -kP$$

This condition is structurally coincides with the refraction-free case, analyzed in [Berngardt and Potekhin(2000)], and corresponds the the well-known Wolf-Bragg condition.

**3.2.2. Integrating over the ray angles.** By integrating (25) over the ray exit angles  $\hat{\Lambda}, \hat{\Lambda}'$  by MSP and using stationary phase condition in form (30), we obtain:

$$(32) \quad P(t, \Delta T) = \int \Phi \left( \vec{R}(\vec{\Lambda}); \vec{k}, \Delta T + S/c - S'/c \right) W_{2,t} \left( \hat{\Lambda}_{SF}, S, \Delta T, S - S' \right) \cdot \\ \cdot |\gamma_2|^2 e^{-i \int_{S'}^S P(k-2k_0 P(\hat{\Lambda}_{SF}, S_1, \omega_0)) dS_1} dS dS' d\vec{k}$$

where

$$(33) \quad W_{2,t} \left( \hat{\Lambda}_{SF}, S, \Delta T, S - S' \right) = W \left( t, 2S, \Delta T, 2\{S - S'\} \right) V_{\Lambda}^{-1} \left( \hat{\Lambda}_{SF}, S, \omega_0 \right) \cdot \\ \cdot V_{\Lambda}^{-1} \left( \hat{\Lambda}_{SF}, S', \omega_0 \right) D_{\Sigma} \left( \hat{\Lambda}_{SF}, S \right)$$

is weight volume that defines spatio-temporal resolution of the technique;  $V_{\Lambda}$  is effective scattering volume;  $\hat{\Lambda}_{SF}$  is stationary point over  $\hat{\Lambda}$ ;

$$\gamma_2 = (2\pi)^{n/2} e^{i\frac{\pi}{4} \text{sgn}(S'')} = 2\pi i$$

is additional multiplier from stationary phase method [Fedoryuk(1989)].

From the initial equation (25) it is obvious that for slowly changing  $\Phi \left( \vec{R}(\hat{\Lambda}_{SF}, S); \right) W \left( t - 2T(\hat{\Lambda}_{SF}, S) \right)$  the stationary points over  $\hat{\Lambda}, \hat{\Lambda}'$  are similar and marked as  $\hat{\Lambda}_{SF}$ , and satisfy the Wolf-Bragg condition (29).

The basic element of the calculations by stationary phase method is the second differential of fast oscillating integrand function  $\psi$ . It defines the integral contribution of the stationary point to the integral, and inverse angular size of the region, making this contribution [Fedoryuk(1989)]:

$$(34) \quad V_{\Lambda} = k \left\| \left\| \frac{\partial^2 \psi}{\partial \hat{\Lambda}_i \partial \hat{\Lambda}_j} \right\| \right\|^{1/2}$$

In geometrical optics the Hessian  $V_{\Lambda}$  can be defined through the product of two main curvature radii  $R_{GM}, R_{Gm}$  [Kravtsov and Orlov(1990)]:

$$(35) \quad V_{\Lambda} = kF^{1/2} = k \{R_{GM}R_{Gm}\}^{1/2}$$

In spectral representation the radar equation (32) becomes:

$$(36) \quad \tilde{P}(t, \omega) = \int \tilde{\Phi} \left( \vec{R}(\vec{\Lambda}); \vec{k}, \nu \right) \tilde{W}_{2,t} \left( \hat{\Lambda}_{SF}, S, \omega - \nu, S - S' \right) \cdot \\ \cdot |\gamma_2|^2 e^{i\nu\{S/c - S'/c\}} e^{-i \int_{S'}^S P(k-2k_0 P(\hat{\Lambda}_{SF}, S_1, \omega_0)) dS_1} dS dS' d\vec{k} d\nu$$

The criterion of applicability of the MSP is a small changes of integrands  $\tilde{\Phi} \left( \vec{R}(\vec{\Lambda}); \vec{k}, \nu \right), \tilde{W}_{2,t} \left( \hat{\Lambda}_{SF}, S, \omega - \nu, S - S' \right)$  at angles about  $V_{\Lambda}^{-1}$  (35), or roughly equivalent, small changes of the integrands at distances of the order Fresnel zone  $\sqrt{\lambda R}$ . This condition has equivalent in

the refraction-free case [Berngardt and Potekhin(2000)]. It should be noted that the smoothness of the refraction index on the characteristic scale of the Fresnel zone is one of the conditions of applicability of geometrical optics [Kravtsov and Orlov(1990)]. Thus, the resulting representation of radar equation (36) is valid almost everywhere, where the original equation (18) is valid and, at the same time, where the average spectral density  $\tilde{\Phi}(\vec{R}(\vec{\Lambda}); \vec{k}, \nu)$  varies smoothly over the spatial variable  $\vec{R}(\vec{\Lambda})$ .

3.2.3. *Integrating the radar equation over the range.* Lets calculate the integral from function (36) that oscillates fast over the  $\Delta S = S - S'$  with the phase  $\varphi$ :

$$(37) \quad \varphi = \nu \Delta S - \int_{S-\Delta S}^S P(k - 2k_0 P(\hat{\Lambda}_{SF}, S_1, \omega_0)) dS_1$$

As it will be shown, it is convenient to analyze the two extreme cases: locally-homogeneous and locally-inhomogeneous one. The integration domain over  $\Delta S$  is limited by the weight volume  $W_{2,t}(\hat{\Lambda}_{SF}, S, \Delta T, \Delta S)$  carrier. For pulse sequences used at SuperDARN radars[Chisham et al.(2007)] this region is defined by elementary sounding pulse duration.

It can be shown that for SuperDARN radars the carrier of  $W_{2,t}$  has a specific shape over  $\Delta S$  - a peak near zero and a few peaks at very large distances  $\Delta S$ . Generally, this volume can be decomposed into the sum of a peaks. For large distances  $\Delta S$  we integrate regions separated by thousands kilometers so the correlation at large  $\Delta S$  and integrals with large  $\Delta S$  can be neglected.

Therefore lets consider the following two limiting cases: when it is a linear function of  $\Delta S$  (it is equivalent to the smallness of second differential of the phase (37) over  $\Delta S$ ) and the integral can be calculated as Fourier transform, and when (37) is very nonlinear function of  $\Delta S$  (when the second differential of the phase (37) over  $\Delta S$  is big enough) and the integral can be calculated with the stationary phase method.

So the (36) calculations can be differed into two classes:

- the locally-homogeneous parts of trajectories (with nearly constant refraction coefficient along the trajectory), at which the scattered signal is accumulated coherently over  $\Delta S$  near zero;
- the locally-inhomogeneous parts of trajectories, at which the main contribution into the integral is made by relatively small area inside the integration region  $\Delta S$ .

So the radar equation (36) will be a sum of two terms - the contributions from locally-homogeneous and from locally-inhomogeneous trajectories.

Locally-homogeneous trajectory case. In the case of locally-homogeneous trajectories the resulting signal is defined by 2D stationary phase method over the ray exit directions  $\hat{\Lambda}$ , and by the Fourier-transform over the radar range  $\Delta S$ . The locally-homogeneous case is equivalent to the refraction-free case [Berngardt and Potekhin(2000)], and 2D stationary phase condition (29) can be considered locally too (31).

It is obvious that background ionosphere can be considered as locally-homogeneous for given sounding pulse only in the case of sufficiently short pulse. However, it should satisfy the narrowband sounding requirement (13), to initial formulas to be valid. When pulse becomes longer and longer there comes a moment when the locally-homogeneous trajectory condition stops working. In this case coherent accumulation of the signal stops and scattered signal amplitude growing stops too. Qualitatively one can suppose that maximal scattered power is reached when the pulse duration and local-homogeneity scale length becomes equal.

The locally-homogeneous trajectory condition (i.e. the maximal size of the region, at which the phase  $\varphi$  (37) can be considered as linear function of  $\Delta S$ ) in the first approximation can be defined from smallness of the second differential of phase (37) as

$$(38) \quad \left( \frac{\Delta R_A}{J_1} \right)^2, \left( \frac{\Delta T_A}{cJ_1} \right)^2 < 1$$

where  $\Delta T_A$  is the elementary sounding pulse duration (defined from the spatial resolution of sounding pulse  $\Delta R_A$ );  $J_1$  - the characteristic scale of quadratic phase changes:

$$(39) \quad J_1 = (2k_0 P \frac{\partial P}{\partial S})^{-1/2}$$

If  $\Delta L$  is a characteristic scale of changes of refractivity index along the trajectory, then  $J_1 \sim \sqrt{\lambda_0 \Delta L}$ .

From the condition of locally-homogeneous trajectory (38) one can see that the requirement is equivalent to small variations of the background refraction coefficient along the trajectory and to short sounding pulses. At these trajectories the radar equation (36) can be significantly simplified. The integration over the  $d(S - S')$  produces Fourier transform of  $W_{2,t}$ :

$$(40) \quad \tilde{P}(t, \omega) = \int \tilde{\Phi} \left( \vec{R}(\vec{\Lambda}); \vec{k}, \nu \right) \cdot |\gamma_2|^2 \tilde{\tilde{W}}_{2,t} \left( \hat{\Lambda}_{SF}, S, \omega - \nu, \left( kP(\hat{\Lambda}_{SF}, S, \omega_0) - 2k_0 P^2(\hat{\Lambda}_{SF}, S, \omega_0) \right) - \nu/c \right) dS d\vec{k} d\nu$$

The narrowband of the sounding signal and spectral density of the irregularities in this case determines the smallness of the wavenumbers region involved into the scattering:

$$(41) \quad \left| kP(\hat{\Lambda}_{SF}, S, \omega_0) - 2k_0P^2(\hat{\Lambda}_{SF}, S, \omega_0) \right| < \Delta\omega/c$$

Taken together, these two conditions (41,31) define space-phase matching for radiowaves and irregularities (Wolf-Bragg condition): the main contribution to the scattering in a smoothly irregular media is produced by irregularities spatial harmonics with wavevectors perpendicular to the wave front of the propagating radio wave, and with the wavenumber nearly equal to the doubled wave number of radiowave propagating in the medium. It is necessary to note that the closer  $P$  (or  $n$ ) to 0, the wider the integration region over  $dk$ . The conditions (41,31) are illustrated at Fig.2A.

To represent (40) as an integral over the space  $d\vec{r}'$ , one needs to calculate Jacobian for the transformation  $dSd\hat{k} \rightarrow d\vec{r}'$ . To simplify the calculations, lets take into account Wolf-Bragg condition ( $d\hat{k} = d\hat{P}$ ) and calculate the following two transformations:  $dSd\hat{P} \rightarrow dSd\hat{\Lambda} \rightarrow d\vec{r}'$

Geometrical interpretation of  $F$  is cross sectional area of the ray [Kravtsov and Orlov(1990)]. From geometrical considerations (see Fig.2B) it is obvious that

$$(42) \quad J_{\hat{P} \rightarrow \hat{\Lambda}} \approx \left\{ \frac{1}{2} \frac{\sigma}{F} \frac{\partial F}{\partial \sigma} \right\}^2$$

It is also clear that  $J_{dSd\hat{\Lambda} \rightarrow d\vec{r}'} = 2n^{-1} \left| \frac{\partial \vec{r}'_i}{\partial \Lambda_j} \right|^{-1} = 2n^{-1} F^{-1}$ . So

$$(43) \quad \begin{aligned} \tilde{P}(t, \omega) = & \int \tilde{\Phi}(\vec{r}'; \vec{k}, \nu) |\gamma_2|^2 k^2 \left\{ \frac{2}{nF} J_{\hat{P} \rightarrow \hat{\Lambda}} \right\} \cdot \\ \cdot \tilde{W}_{2,t}(\hat{\Lambda}_{SF}(\vec{r}'), S(\vec{r}'), \omega - \nu, & \left( kP(\hat{\Lambda}_{SF}(\vec{r}'), S(\vec{r}'), \omega_0) - 2k_0P^2(\hat{\Lambda}_{SF}(\vec{r}'), S(\vec{r}'), \omega_0) \right) - \nu/c) \end{aligned}$$

where  $W_{2,t}(\hat{\Lambda}_{SF}, S, \Delta T, S - S')$  is defined by (33).

The additional spatial multiplier  $\left\{ \frac{2}{nF} J_{\hat{P} \rightarrow \hat{\Lambda}} \right\}$  is relatively smooth over the space (except the caustics regions, where it becomes infinite). For refraction-free case it is equal to  $\frac{2}{r^2}$ , and the radar equation (43) becomes similar to the obtained in [Berngardt and Potekhin(2000)].

In Fig.3 are illustrated the locally-homogeneous areas for model ionosphere. The figure shows that such basic areas are: field caustics associated with reflection (170-270km); area corresponding F2-peak (270km) and E-peak (120 km); and the region of linear propagation out of the ionosphere (area 0-90km altitude).

Locally-inhomogeneous trajectory case. With increase of the variations of the refractivity index along the trajectory or/and increase of the sounding pulse duration the situation changes gradually. In this case the phase (37) can not be considered as a linear function of  $\Delta S$ , and

Fourier transform approximation can not be used, and one need to use other approximate methods to calculate fast oscillating integral (36).

In the case of locally-inhomogeneous trajectories integration of the radar equation (36) over  $\Delta S$  can be done by using stationary phase method. One also can not use the local condition for stationary point (31) instead of the integral one (30). This mean that the stationary point will be defined from 3D structure of the integral.

Calculating the position of the stationary point  $\hat{\Lambda}_{SF}, S_{SF}$  over  $S$  and  $S'$  separately in (36) gives the following integral conditions for stationary phase:

$$(44) \quad \begin{cases} \int_{S-\Delta S_W}^S \vec{k} \left( \frac{\partial \vec{P}}{\partial \Lambda} \right)_{\perp \vec{P}} dS_1 = 0 \\ \vec{k} \vec{P}(\hat{\Lambda}_{SF}, S_{SF}) - 2k_0 P^2(\hat{\Lambda}_{SF}, S_{SF}) - \nu/c = 0 \end{cases}$$

In the case when the stationary point  $S_{SF}$  is a single one and is within the carrier of  $W(S)$   $[S - \Delta S_W, S]$  for given  $t$  it makes a big contribution into integral (36). In other cases the contribution is small. It should be noted that multiplier outside the carrier of  $W(S)$   $\int_0^{S-\Delta S_W} \vec{k} \left( \frac{\partial \vec{P}}{\partial \Lambda} \right)_{\perp} dS_1$  can be removed out the integral sign. So actually the MSP (44) is calculated over the carrier of  $W(S)$ .

In this case both stationary points (for  $S$  and  $S'$ ) coincide and integral will lead to the  $W(\Delta S = 0)$ , and the expression (36) becomes:

$$(45) \quad P(t, \Delta T) = \int \tilde{\Phi} \left( \vec{R}(\vec{\Lambda}_{SF}); \vec{k}, \Delta T \right) W \left( t, 2T(\vec{\Lambda}_{SF})c, \Delta T, 0 \right) \cdot |\gamma_2 \gamma_1|^2 J_1^2 V_{\Lambda}^{-2}(\vec{\Lambda}_{SF}, \omega_0) D_{\Sigma}(\dots) d\vec{k}$$

$$(46) \quad \tilde{P}(t, \omega) = \int \tilde{\Phi} \left( \vec{R}(\vec{\Lambda}_{SF}); \vec{k}, \nu \right) \tilde{W} \left( t, 2T(\vec{\Lambda}_{SF})c, \omega - \nu, 0 \right) \cdot |\gamma_2 \gamma_1|^2 J_1^2 V_{\Lambda}^{-2}(\vec{\Lambda}_{SF}, \omega_0) D_{\Sigma}(\dots) d\vec{k} d\nu$$

where

$$\gamma_1 = (2\pi)^{1/2} e^{i\frac{\pi}{4}} = \sqrt{2\pi}i$$

is additional multiplier from stationary phase method [Fedoryuk(1989)];  $J_1$  is defined by (39).

Taking into account the same considerations, as for analysis formula (40), we can obtain:

$$(47) \quad P(t, \omega) = \int \tilde{\Phi} \left( \vec{R}(\hat{\Lambda}_{SF}, S_{SF}(\hat{k}_{SF}k)); \hat{k}_{SF}k, \nu \right) \tilde{W}_{2,t} \left( \hat{\Lambda}_{SF}, T(\hat{\Lambda}_{SF}, S_{SF}(\hat{k}_{SF}k))c, \omega - \nu, 0 \right) \cdot |\gamma_2 \gamma_1|^2 J_1^2(\hat{\Lambda}_{SF}, S_{SF}(\hat{k}_{SF}k)) D_{\Sigma}(\dots) J_{\hat{P} \rightarrow \hat{\Lambda}} k^2 dk d\hat{\Lambda} d\nu$$

To estimate the relation between contributions of locally-homogeneous (40) and locally-inhomogeneous (47), we can estimate  $d\vec{r} \sim \left(\frac{S}{2}\right)^2 \Delta R_A d\hat{\Lambda}$  in (40). So the relation can be estimated as:

$$\frac{P_{inhom}(t, \omega)}{P_{hom}(t, \omega)} \approx \frac{J_1^2 J_{\hat{P} \rightarrow \hat{\Lambda}} \frac{\Delta \omega_A}{nc} \Delta \omega_A}{\left(\frac{S}{2}\right)^2 \left\{ \frac{2}{nF} J_{\hat{P} \rightarrow \hat{\Lambda}} \right\} \Delta R_A^2 \frac{\Delta \omega_A}{nc} \Delta \omega_A} \approx \frac{J_1^2}{\{\Delta R_A\}^2}$$

So the energy of the scattered signal in locally-homogeneous case approximately  $(\Delta R_A/J_1)^2$  times higher then in locally-inhomogeneous case.

In Fig.4A shown the value of  $J_1^2/(\Delta R_A)^2$  for locally-homogeneous (=0dB, yellow areas), and for locally-inhomogeneous trajectories (red and blue colors). The calculations for Fig.4A are made with the reference model ionosphere (IRI-2012) and typical frequency and duration of SuperDARN sounding signal.

In Fig.4A shown that the regions with locally-inhomogeneous trajectories (red and blue) are located between the E- and F-maximum and expected to produce scattering about 10-15dB less powerful than the region of locally-homogeneous trajectories. Because of the field-aligned scatterers (studied by SuperDARN radars) produce powerful aspect scattering these areas look still important for future consideration.

#### 4. BISTATIC SOUNDING

To analyze the bistatic sounding we assume, by analogy with [Berngardt and Potekhin(2002)] that trajectories of the transmitted and received signal are spaced far enough from each other. This means that the angle between the incident and scattered ray bigger than the angular size of the area of the stationary phase (35). The case of smaller angle the problem degenerates into the monostatic case, already analyzed (45). It should be noted that in presence of refraction this condition in general is not connected with the relative position of transmitter and receiver (in opposite to refraction-free situation [Berngardt and Potekhin(2002)]), but is connected only with the angle between the trajectories of transmitted and scattered signal at the point of scattering.

**4.1. Single trajectory pair: initial equation.** Lets analyze the case of single trajectory pair: there is only one propagation path from the transmitter to scattering point, and only one path from receiver to the scattering point. And they differ.

We consider the scattered signal as the integral over the ray coordinates  $\vec{\Lambda}_t$  associated with the transmitter and over the spatial coordinates  $\vec{r}$  of the scatterer position. In this case, the scattering signal (16) leads to the following correlation function  $P(t, \Delta T)$ :

(48)

$$\begin{aligned}
P(t, \Delta T) &= \int \tilde{\Phi}(\vec{r}; \vec{k}, \Delta T + T_t - T'_t) \cdot \\
\cdot W(t, \{T_r + T_t\} c, \Delta T, \{(T_r + T_t) - (T'_r + T'_t)\} c) &D(\vec{\Lambda}_r, \vec{\Lambda}_t, \omega_0) D(\vec{\Lambda}'_r, \vec{\Lambda}'_t, \omega_0) \cdot \\
\cdot e^{i\vec{k}(\vec{r} - \vec{r}')} e^{ik_0\Psi(\vec{\Lambda}_r, \vec{\Lambda}_t)} e^{-ik_0\Psi(\vec{\Lambda}'_r, \vec{\Lambda}'_t)} & \cdot \\
\cdot \delta(\vec{r} - \vec{R}(\vec{\Lambda}_t)) \delta(\vec{r}' - \vec{R}(\vec{\Lambda}'_t)) &F^{-1}(\vec{\Lambda}_r(\vec{r})) F^{-1}(\vec{\Lambda}'_r(\vec{r}')) d\vec{\Lambda}_t d\vec{r} d\vec{\Lambda}'_t d\vec{r}' d\vec{k}
\end{aligned}$$

#### 4.2. Single trajectory pair: obtaining of the radar equation.

Integrating delta-functions over the  $\vec{\Lambda}_t, \vec{\Lambda}'_t$  in (48) will result to  $\vec{\Lambda}_t(\vec{r})$  and  $\vec{\Lambda}'_t(\vec{r}')$  functions under the integral and corresponding Jacobian  $F^{-1}$ :

(49)

$$\begin{aligned}
P(t, \Delta T) &= \int \tilde{\Phi}(\vec{r}; \vec{k}, \Delta T + T_t - T'_t) \\
W(t, \{T_r + T_t\} c, \Delta T, \{(T_r + T_t) - (T'_r + T'_t)\} c) &D(\vec{\Lambda}_r, \vec{\Lambda}_t, \omega_0) D(\vec{\Lambda}'_r, \vec{\Lambda}'_t, \omega_0) \\
e^{i\vec{k}(\vec{r} - \vec{r}')} e^{ik_0\Psi(\vec{\Lambda}_r, \vec{\Lambda}_t)} e^{-ik_0\Psi(\vec{\Lambda}'_r, \vec{\Lambda}'_t)} & \\
|\gamma_3|^2 F_4^{-1}(\vec{r}(\vec{k}), \vec{r}'(\vec{k})) &d\vec{r} d\vec{r}' d\vec{k}
\end{aligned}$$

where

$$(50) \quad F_4(\vec{r}, \vec{r}') = F(\vec{\Lambda}_r(\vec{r})) F(\vec{\Lambda}'_r(\vec{r}')) F(\vec{\Lambda}_t(\vec{r})) F(\vec{\Lambda}'_t(\vec{r}'))$$

$$\gamma_3 = (2\pi)^{n/2} e^{i\frac{\pi}{4} \text{sgn}(S'')} = (2\pi i)^{3/2}$$

is additional multiplier from MSP [Fedoryuk(1989)].

We can integrate the expression (49) over the  $d\vec{r}$  and  $d\vec{r}'$  by MSP separately.

Integrating over  $d\vec{r}$  will lead to the following stationary phase condition:

$$(51) \quad \vec{k} + k_0 \frac{\partial}{\partial \vec{r}} \psi_t(\vec{\Lambda}_t) + k_0 \frac{\partial}{\partial \vec{r}} \psi_r(\vec{\Lambda}_r) = 0$$

Taking into account that  $\vec{r} = \vec{R}_r(\vec{\Lambda}_r) = \vec{R}_t(\vec{\Lambda}_t)$  and taking into account the properties of hamiltonian trajectories (10), the stationary phase condition will take the clear look that shows the selective properties of the scattering:

$$(52) \quad \vec{k} + k_0 \vec{P}_t(\vec{\Lambda}_t) + k_0 \vec{P}_r(\vec{\Lambda}_r) = 0$$

Doing the same over  $d\vec{r}'$  and assuming the stationary point  $\vec{r}^0$  to be only one for each  $\vec{k}$  we can transform the radar equation (49) to the form:

(53)

$$P(t, \Delta T) = \int \tilde{\Phi}(\vec{r}; \vec{k}, \Delta T) W(t, (T_r + T_t) \frac{c}{2}, \Delta T, 0) \\ V_R^2(\vec{r}_{SF}) D_\Sigma(\vec{\Lambda}_r, \vec{\Lambda}_t, \vec{\Lambda}_r, \vec{\Lambda}_t, \omega_0) |\gamma_3|^2 F_4^{-1/2}(\vec{r}(\vec{k}), \vec{r}(\vec{k})) d\vec{k}$$

From qualitative considerations, the effective scattering volume  $V_R$  should be close to that obtained for refraction-free case [Berngardt and Potekhin(2002)], but instead of product  $R_t R_s$  there should be the curvature radii (as previously shown, they will automatically appear in the two-dimensional stationary phase method over the angles (35)):

(54)

$$V_R \approx \{R_{GM,t} R_{Gm,t} R_{GM,r} R_{Gm,r}\}^{1/2} k_0^{-3/2} (\vec{P}_t \times \vec{P}_r)^{-1} (R_t + R_r)^{-1/2}$$

The effective scattering volume  $V_R$  is determined as:

(55)

$$V_R = |\aleph|^{-1/2}$$

where

(56)

$$\aleph = \left\{ \frac{\partial}{\partial r_j} \{k_0 P_{t,i} + k_0 P_{r,i} + k_i\} \right\}_{\vec{r}=\vec{r}_0}$$

It is necessary to note that this condition corresponds to locally-homogeneous trajectories. As can be seen from Fig.3, in the E-layer (heights 100-130 km) both trajectories (transmitter-scatterer and scatterer-receiver) can be considered as locally-homogeneous ones, and correspondingly one can use a local formulation of the Wolf-Bragg conditions (52). For the rest of the points, in which the trajectory of locally-inhomogeneous, this approach is not entirely correct and should be investigated separately. Expectedly, that in this case the effective scattering volume will be less powerful, and will be determined by the differential of the refraction index along the propagation trajectory (similar to the case of the monostatic scattering).

It is easy to show that in a refraction-free case the (54) transforms to the formulas obtained in [Berngardt and Potekhin(2002)].

From the formulas (52,56) it is obvious that

(57)

$$\aleph = \frac{\partial k_i(\vec{r})}{\partial r_j}$$

are the Lamé coefficients for the transition to the coordinate system associated with the wave vectors  $\vec{k}$  from the coordinate system associated with spatial vectors of stationary points  $\vec{r}$  (in the case that this transformation is bijection).

This means that in case of bijection  $\vec{k} \rightarrow \vec{r}$  the integral over stationary points in the wave vectors space (53) can be represented

as an integral over space  $\vec{r}'$ , where the exact expression for  $V_R$  (54) is not important:

$$(58) \quad P(t, \Delta T) = \int \tilde{\Phi}(\vec{r}, t - T_t; \vec{k}(\vec{r}), \Delta T) W(t, (T_r + T_t)c, \Delta T, 0) |\gamma_3|^2 D_\Sigma(\vec{\Lambda}_r, \vec{\Lambda}_t, \vec{\Lambda}_r, \vec{\Lambda}_t, \omega_0) F_4^{-1/2}(\vec{r}, \vec{r}') d\vec{r}'$$

In this expression explicitly highlighted the dependence of the power of the scattered signal from the scattering angle (52) (in the refraction-free case it is determined by the distance between the transmitter and receiver) and from the Gaussian curvature of the beams  $F_4^{1/2}$  (in the refraction-free case it is determined by the distance to the investigated volume from the receiver and transmitter, respectively). So, the effective weight volume  $V_R$  is defined by Jacobian for the transition from the wave vector  $\vec{k}$  space to usual space  $\vec{r}$ , and is not important for spatial integral representation (58). The shape of  $V_R$  is important when one estimate the homogeneity scale for the media, necessary for the obtained formulas to be valid. Also its exact shape should be important when the scattering is produced by a single spatial harmonic (for example, during radioacoustical sounding of the ionosphere [Lataitis(1992)]) and wavevector representation (53) may be more convenient.

**4.3. Multiple trajectories pairs.** If there are exist multiple propagation trajectories from the transmitter to the scatterer ( $M$  trajectories) and multiple paths from the scatterer to the receiver ( $N$  trajectories) the radar equation becomes more complex than (58).

In this case integration over  $\vec{\Lambda}_t, \vec{\Lambda}'_t$  in (49) will remove the delta function, but produce some cross-sums over the trajectories, replacing the function arguments with the corresponding functions  $\vec{\Lambda}_{t,m}(\vec{r}), \vec{\Lambda}'_{t,m'}(\vec{r}'), \vec{\Lambda}_{r,n}(\vec{r}), \vec{\Lambda}'_{r,n'}(\vec{r}')$  (calculated based on the delta-function arguments), where indexes  $n, n', m, m'$  mark trajectories :

$$(59) \quad P(t, \Delta T) = \sum_{n,n' \in N, m,m' \in M} \int \tilde{\Phi}(\vec{r}, t - T_{t,m}; \vec{k}, \Delta T + T_{t,m} - T'_{t,m'}) \cdot W(t, (T_{r,n} + T_{t,m})c, \Delta T, ((T_{r,n} + T_{t,m}) - (T'_{r,n'} + T'_{t,m'}))c) D_\Sigma(\vec{\Lambda}_{r,n}, \vec{\Lambda}_{t,m}, \vec{\Lambda}'_{r,n'}, \vec{\Lambda}'_{t,m'}, \omega_0) \cdot F_{4,n',m,m'}^{-1/2}(\vec{r}', \vec{r}') \cdot e^{i\vec{k}(\vec{r}-\vec{r}')} e^{ik_0\Psi_{n,m}(\vec{\Lambda}_{r,n}, \vec{\Lambda}_{t,m})} e^{-ik_0\Psi_{n',m'}(\vec{\Lambda}'_{r,n'}, \vec{\Lambda}'_{t,m'})} d\vec{r}' d\vec{r}' d\vec{k}$$

where

$$(60) \quad F_{4,n',m,m'}(\vec{r}, \vec{r}') = F(\vec{\Lambda}_{r,n}(\vec{r})) F(\vec{\Lambda}'_{r,n'}(\vec{r}')) F(\vec{\Lambda}_{t,m}(\vec{r})) F(\vec{\Lambda}'_{t,m'}(\vec{r}'))$$

In this case the condition of the stationary phase for each pair of trajectories will take an already discussed form (52):

$$(61) \quad \vec{k} + k_0 \vec{P}_t(\vec{\Lambda}_{t,m}) + k_0 \vec{P}_r(\vec{\Lambda}_{r,m}) = 0$$

Assuming the stationary point  $\vec{r}_{n,m}^0$  to be only one for each given  $\vec{k}$  and for each selected unordered pair of trajectories  $(n, m)$  the radar equation will take the form:

$$(62) \quad \begin{aligned} P(t, \Delta T) = & \sum_{n,n' \in N, m, m' \in M} \int \tilde{\Phi}(\vec{r}, t - T_{t,m}; \vec{k}, \Delta T + T_{t,m} - T'_{t,m'}) \cdot \\ & \cdot W(t, (T_{r,n} + T_{t,m})c, \Delta T, ((T_{r,n} + T_{t,m}) - (T'_{r,n'} + T'_{t,m'}))c) D_{\Sigma}(\vec{\Lambda}_{r,n}, \vec{\Lambda}_{t,m}, \vec{\Lambda}'_{r,n'}, \vec{\Lambda}'_{t,m'}, \omega_0) \cdot \\ & \cdot |\gamma_3|^2 F_{4,n,n',m,m'}^{-1}(\vec{r}(\vec{k}), \vec{r}'(\vec{k})) \\ & \cdot e^{i\vec{k}(\vec{r}_{n,m}^0 - \vec{r}'_{n',m'})} e^{ik_0\Psi(\vec{\Lambda}_{r,n,m}, \vec{\Lambda}_{t,n,m})} e^{-ik_0\Psi(\vec{\Lambda}'_{r,n',m'}, \vec{\Lambda}'_{t,n',m'})} V_{R,n,m}^2 d\vec{k} \end{aligned}$$

When transforming to the space coordinate system the effective weight volume  $V_{R,n,m}$  disappears, because it is equal to the Jacobian of the transition from one coordinate system  $(\vec{k})$  to another  $(\vec{r})$  (55,57):

$$(63) \quad \begin{aligned} P(t, \Delta T) = & \sum_{n,n' \in N, m, m' \in M} \int \tilde{\Phi}(\vec{r}, t - T_{t,m}; \vec{k}, \Delta T + T_{t,m} - T'_{t,m'}) \cdot \\ & \cdot W(t, (T_{r,n} + T_{t,m})c, \Delta T, ((T_{r,n} + T_{t,m}) - (T'_{r,n'} + T'_{t,m'}))c) D_{\Sigma}(\vec{\Lambda}_{r,n}, \vec{\Lambda}_{t,m}, \vec{\Lambda}'_{r,n'}, \vec{\Lambda}'_{t,m'}, \omega_0) \cdot \\ & \cdot |\gamma_3|^2 F_{4,n,n',m,m'}^{-1/2}(\vec{r}, \vec{r}') e^{i\vec{k}(\vec{r}_{n,m}^0 - \vec{r}'_{n',m'})} e^{ik_0\Psi(\vec{\Lambda}_{r,n,m}, \vec{\Lambda}_{t,n,m})} e^{-ik_0\Psi(\vec{\Lambda}'_{r,n',m'}, \vec{\Lambda}'_{t,n',m'})} d\vec{r} \end{aligned}$$

## 5. RESULTING SUPERDARN RADAR EQUATION

In Fig.4B are shown the geometrooptical trajectories in a model of spherically stratified ionosphere. From the figure it is seen that within the region bounded by the caustics, there is a region in which it is possible to reach the same point by multiple trajectories (In Fig.4B the region is limited by the black triangle). The upper limit for this region is the caustic associated with reflection from the ionosphere by the lower ray, the left border is the caustic associated with the boundary of the dead zone (i.e. ground backscatter position), and the right border is the trajectory with the lowest possible elevation angle.

Qualitative analysis has shown in the simple model case that the number of trajectories to the each point, lying inside this region can be two or three: the first is direct propagation trajectory, the second is the trajectory reflected from the the ionosphere by lower ray, and the last one is the trajectory reflected from the ionosphere by the upper ray. Thus, in this area the case is possible when the signal propagates towards and backwards the scatterer by substantially different trajectories. The limit case for this effect is the area of caustics, where to the same

point at the same time comes a large number of rays, that leads to significant gain of the signal.

In this paper we do not consider the caustic regions, but the area inside the area bounded by the caustics can be considered.

The region, where all the 3 rays exist and intersect is marked by blue triangle in Fig.4B. The region where at least two trajectories exists is marked by black triangle. So the scattering problem in the region can be considered as equivalent of bistatic sounding problem.

In this case of several possible propagation trajectories from the transmitter to the scatterer a situation arises that is equivalent to the situation of bistatic sounding (62,63). This case does not arise in the refraction-free case, since in refraction-free case there is only single trajectory exists between two points.

Lets consider the case of multiple trajectories in case of monostatic sounding that is shown in Fig.4C. It can be seen that on the trajectories, allowing the reflection from the ionosphere (i.e., at distances above 0.5 hop) there can be a few (at least two) signal propagation trajectories to the scattering point. The trajectory marked with 1 is the path of direct propagation (reflection-free trajectory). The paths marked by 2,3 are the trajectories that includes reflection from the ionosphere.

Lets obtain the radar equation in the case when all three trajectories exists. When analyzing the signal autocorrelation function it is convenient to analyze the simplest case, valid for SuperDARN radars.

It is the case when selection over the delays is made with short enough sounding pulses, spaced by large enough delay between each other. The pulses are short enough to differ two trajectories by delay:  $(T_{r,n} + T_{t,m}) - (T'_{r,n'} + T'_{t,m'}) > \Delta T_A$  where unordered pairs  $(n, m) \neq (n', m')$ . This condition also compensate the additional caustic phase, that arise when wave reflects from the ionosphere, and the caustic phase does not affect on resulting radar equation.

In this case the short sounding pulse provides selection of correlating trajectories when the difference between propagation delays is larger than pulse duration. The final radar equation, after taking into account symmetry considerations, becomes:

$$\begin{aligned}
(64) \quad & \tilde{P}(t, \omega) = \sum_{n \in N, |J_1/\Delta R_A| > 1} \int \tilde{\Phi}(\vec{r}; -\hat{P}_n^H(\vec{r})k, \nu) A_n^H(\vec{r}) \cdot \\
& \cdot \tilde{W}_{2,t}(\hat{\Lambda}_n^H(\vec{r}), S_n(\vec{r}), \omega - \nu, (kP(\vec{r}, \omega_0) - 2k_0P^2(\vec{r}, \omega_0)) - \nu/c) k^2 dk d\nu d\vec{r} + \\
& + \int_{|J_1/\Delta R_A| < 1} \tilde{\Phi}(\vec{R}(\hat{\Lambda}, S_{SF}(\hat{k}_{SF}^I k)); \hat{k}_{SF}^I k, \nu) A^I(\vec{R}(\hat{\Lambda}, S_{SF}(\hat{k}_{SF}^I k))) \cdot \\
& \cdot \tilde{W}_{2,t}(\hat{\Lambda}, S_{SF}(\hat{k}_{SF}^I k), \omega - \nu, 0) k^2 dk d\nu d\hat{\Lambda} + \\
& + \sum_{n, m \in N, n > m} \int \tilde{\Phi}(\vec{r}; \vec{k}_{n,m}(\vec{r}), \nu) 2(1 + \cos(\nu(T_m(\vec{r}) - T_n(\vec{r})))) \cdot \\
& \cdot A_{n,m}(\vec{r}) \tilde{W}(t, c(T_n(\vec{r}) + T_m(\vec{r})), \omega - \nu, 0) d\nu d\vec{r}
\end{aligned}$$

where:

$$\begin{aligned}
(65) \quad & A_n^H(\vec{r}) = (2\pi)^2 k_0^4 \left\{ \frac{2}{PF} J_{\hat{P} \rightarrow \hat{\Lambda}} \right\} \\
& A^I(\vec{r}) = (2\pi)^3 k_0^4 \left| g_r^*(\hat{\Lambda}, \omega_0) g_t(\hat{\Lambda}, \omega_0) \right|^2 J_1^2 J_{\hat{P} \rightarrow \hat{\Lambda}} \\
& A_{n,m}(\vec{r}) = \frac{(2\pi)^3 k_0^4}{F_n F_m} \left| g_r^*(\hat{\Lambda}_n(\vec{r}), \omega_0) g_t(\hat{\Lambda}_m(\vec{r}), \omega_0) \right|^2
\end{aligned}$$

are the multipliers that strongly affected by background ionosphere and define power changes due to geometroptical and focusing effects.

Here all the obvious arguments are hidden, and  $J_1, J_{\hat{P} \rightarrow \hat{\Lambda}}, \tilde{W}_{2,t}, \tilde{W}, F$  and  $V_\Lambda$  are defined by (39,42,33,22,3,35) correspondingly.  $N$  is the maximal number of trajectories to reach the same point at the same time. In analyzed case  $N = [1, 2, 3]$ : reflection-free ray[1], lower ray[2] and Pedersen ray[3] (see Fig.4C).

The radar equation (64) does not contain any oscillating terms and is convenient for qualitative analysis or numerical simulations of scattering process. In most cases,  $\Phi(k)$  can be considered a smooth function of  $k$  at scale  $\Delta\omega/(cP)$  and radar equation (64) can be simplified even more.

The first two terms in (64) are associated with the propagating of the signal over the identical trajectories towards the scatterer and backwards. For any given scattering point whether first or second term will be valid, because the integration of the first term is made over the spatial area where  $|J_1/\Delta R_A| > 1$  (locally-homogeneous trajectory part), and second - over the spatial area with  $|J_1/\Delta R_A| < 1$  (locally-inhomogeneous trajectory part).

The first term in the radar equation (64) corresponds to the stationary points located at locally-homogeneous trajectories (which is traditionally investigated in SuperDARN tasks or in refraction-free case by VHF radars), the stationary point is marked by  $H$  upper index and is defined by (31). It's usage is limited by locally-homogeneous condition  $|J_1/\Delta R_A| >$

1, for SuperDARN case it is valid for very limited regions, including ionospheric E-layer and F-layer maximums (see Fig.3). Exit angle  $\hat{\Lambda}_n^H(\vec{r})$ , group path  $S_n(\vec{r})$  and wave direction  $\hat{P}_n^H(\vec{r})$ , as well as  $A_n^H(\vec{r})$  value, that correspond to investigated point  $\vec{r}$  can be calculated using ray-tracing technique (10). In refraction-free case this term transforms to the refraction-free radar equation [Berngardt and Potekhin(2000)].

The second term in the radar equation (64) corresponds to the stationary points located at locally-inhomogeneous trajectories, the stationary point is marked by  $I$  upper index and is defined by (44). It's usage is limited by locally-inhomogeneous condition  $|J_1/\Delta R_A| < 1$ . For SuperDARN case it is valid for most part of the F-layer ionosphere (see Fig.3). This case has no equivalent in refraction-free situation. To calculate it one need to find the point with most intensive scattering  $S_{SF}(\hat{\Lambda}, k)$  that is defined by system (44). It looks complex task, but the simplest way to estimate it, is to calculate the wavevector direction  $\hat{k}_{SF}^I$  that in average is perpendicular to wavefront according to the first condition in (44) for given exit angle  $\hat{\Lambda}$  and over weight volume  $W(..)$

size: 
$$\int_{ct/2-\Delta R_A}^{ct/2+\Delta R_A} \hat{k}_{SF}^I \left( \frac{\partial \vec{P}}{\partial \hat{\Lambda}} \right)_{\perp \vec{P}} dS_1 = 0 .$$
 Then one can numerically find

the point  $S_{SF}$ , at which the Wolf-Bragg condition (second condition in (44),  $k \hat{k}_{SF}^I \vec{P}(\hat{\Lambda}, S_{SF}) - 2k_0 P^2(\hat{\Lambda}, S_{SF}) - \nu/c = 0$ ) is satisfied for given wavenumber  $k$ , exit angle  $\hat{\Lambda}$  and calculated average wavefront perpendicular  $\hat{k}_{SF}^I$ . It is important to note, that  $S_{SF}$  should be  $\in [ct/2 - \Delta R_A, ct/2 + \Delta R_A]$ , or integral becomes neglectable because the carrier of weight volume  $W(...)$ . The  $A^I(\vec{r})$  value and group delay  $T_n(\vec{r})$  to the investigated point can be calculated during ray-tracing.

The third term (cross-sums) in the radar equation (64) is associated with propagation towards the scatterer over one trajectory and backwards to the receiver over another trajectory, and is an equivalent of bistatic scattering[Berngardt and Potekhin(2002)]. The stationary point is defined by (61). Wavevector  $\vec{k}_{n,m}(\vec{r})$  can be found using Wolf-Bragg condition (61) by ray-tracing technique (10) over two different trajectories  $n, m$  to the investigated point  $\vec{r}$ .  $A_{n,m}(\vec{r})$  value, group delays  $T_n(\vec{r}), T_m(\vec{r})$  and exit angles  $\Lambda_n(\vec{r}), \Lambda_m(\vec{r})$  to the investigated point can be also calculated during ray-tracing. This case does not arise in refraction-free situation. It should be noted that existence of the third term was considered and discussed for a static scatterer in [Kravtsov and Namazov(1980)].

To take into account a weak absorption  $\chi$  during radiowave propagation, for example in D-layer [Ginzburg(1970), Settini et al.(2014), Settini et al.(2015)], one should include the multiplier  $e^{-2 \int_0^{ct/n} \chi(\vec{R}(\hat{\Lambda}_n, S', \omega_0)) dS'}$  into each of  $A_n^H(\vec{r}), A^I(\vec{r})$  and the multiplier  $e^{-\int_0^{ct/n} \chi(\vec{R}(\hat{\Lambda}_n, S', \omega_0)) dS' - \int_0^{ct/m} \chi(\vec{R}(\hat{\Lambda}_m, S', \omega_0)) dS'}$  into  $A_{n,m}(\vec{r})$ .

## 6. DISCUSSION AND CONCLUSION

Based on hamiltonian optics approach and ray representation of Green's function we obtained the scalar radar equation (64) that is suitable for taking into account the refraction effects in SuperDARN data (autocorrelation functions of the received signals) obtained by these radars within the first hope distances (i.e. before scattering of the signal from the ground). The main conclusions from this radar equation are the following.

1. The radar equation shows that the integral kernel that relates the measured correlation function of the signal with the correlation function of the ionospheric irregularities, is the weight volume (or ambiguity function)  $W(\dots)$ (22), the widely studied for refraction-free case [Lehtinen(1986), Berngardt and Potekhin(2000), Berngardt and Potekhin(2002)]. This weight volume is defined by the shape of a sounding signal and by signal processing techniques. Radar equation (64) is linear over  $W(\dots)$ , so making any linear transformation of the scattered signal correlation function or spectral power leads just to equivalent transformation of the weight volume  $W(\dots)$  [Lehtinen(1986), Berngardt and Kushnarev(2013)] and does not affect on the structure of the radar equation. This allows, for example, to prove the validity of using at SuperDARN radars the signal processing techniques and sounding sequences, initially developed for refraction-free cases ([Farley(1972), Berngardt et al.(2015b)], etc.).

2. The radar equation shows that the spatial harmonics that produce the main contribution to the scattering signal are determined by the local wave vector and satisfy to the Wolf-Bragg condition (31,41). This is very close to refraction-free case [Berngardt and Potekhin(2000), Berngardt and Potekhin(2002)]. This also confirms with the results of [Gillies et al.(2011)], and allows to take it into account refraction effects in the velocities of ionospheric irregularities measured by SuperDARN radars.

3. In contrast to the refraction-free case, the refraction significantly affects the scattered signal amplitude. At first, this effect leads to amplitude changes related to the focusing of the signal during propagation (multipliers  $F^{-1/2}$ ) in the region of the scattering. The second effect is associated with attenuation of the scattered signal due changing the wave length of sounding signal at intervals of the length of the sounding pulse (parameter  $J_1$  in the equation).

4. Obtained radar equation is not exactly correct for the Pedersen rays after the point of their reflection. This is associated with considerable frequency distortion of the propagating signal in this area ( higher-frequency components are not reflected by the ionosphere) and, as a consequence, the inapplicability of the undistorted signal propagation model.

5. The highest amplitude of the scattered signal occurs in regions close to the areas of focusing, and in the areas where the refractive index varies slightly along the propagation trajectories. These areas

correspond to the caustic trajectories, the areas near the local maximum of the electron density (Pedersen rays) and the areas where the ionospheric refraction can be neglected (the areas below the E-layer). Outside these areas, the amplitude of the scattered signal is reduced and can be compensated only by a high aspect dependence of scattering irregularities. The maximal scattering amplitude at Pedersen ray have been detected, for example, as a result of interpretation of the first Russian-Ukrainian experiment using EKB radar and UTR-2 radiotelescope [Berngardt et al.(2015a)].

6. When signal propagates in an inhomogeneous ionosphere there are areas in which the signal reaches the point of scattering by several (two or more) different trajectories simultaneously. We modeled the orthogonality conditions of wave vector to the magnetic field, important for scattering by field-aligned irregularities, with taking into account the structure of the Earth magnetic field (IGRF reference model used) and model ionosphere (IRI-2012 reference model used). Modeling shows that the bistatic mechanism should be important for polar radars looking equatorward (see Fig.5). In spite in this case the angle between propagation trajectory and magnetic field is far from orthogonality (about 50 degrees), the wavevector of the scattering irregularities  $\vec{k}$  is orthogonal to magnetic field  $\vec{B}$ . This mechanism allows to interpret strong field-aligned scattering even at very high aspect angles between trajectory and magnetic field.

7. The first two mechanisms can be considered as a result of monostatic scattering similar to the refraction-free case [Tatarsky(1967), Ishimaru(1978), Berngardt and Potekhin(2000)]. The third mechanism should be considered as an equivalent of bistatic sounding in refraction-free case [Tatarsky(1967), Ishimaru(1978), Berngardt and Potekhin(2002)]. This case apparently has not been considered in SuperDARN tasks. The existence of a third mechanism has been proposed and investigated for the case of stationary irregularities for example in [Kravtsov and Namazov(1980)]. It should be noted that in the last case, despite the possibility of differencing the trajectories over the time of arrival, the measured spectrum is distorted by  $2(1 + \cos(\nu(T_m - T_n)))$  multiplier due to trajectory pairs with exactly the same group length. Conversely, the existence of such distortions in the received signal spectral power allows to detect the multiple propagation case.

## 7. ACKNOWLEDGMENTS

The work of OB and AP has been done under support of FSR program II.12.2.2. The work of KK has been done under support of RFBR grant #16-05-01006a. The numerical simulations have been performed with High-performance computing cluster "Academician V.M. Matrosov" (<http://hpc.icc.ru>)

## REFERENCES

- [Babich and Buldyrev(1978)] Babich, V. M. and Buldyrev, V. S. (1978). *Asymptotic Methods in Diffraction Problems for Short Waves (in russian)*. Nauka, Moscow.
- [Baker et al.(2007)] Baker, J., Greenwald, R., Ruohoniemi, J., Oksavik, K., Gjerloev, J. W., Paxton, L. J., and Hairston, M. (2007). Observations of ionospheric convection from the Wallops SuperDARN radar at middle latitudes. *Journal of Geophysical Research: Space Physics*, 112:A01303.
- [Berngardt and Potekhin(2000)] Berngardt, O. and Potekhin, A. (2000). Radar equations in the radio wave backscattering problem. *Radiophysics and Quantum Electronics*, 43(6):484–492.
- [Berngardt and Potekhin(2002)] Berngardt, O. I. and Potekhin, A. P. (2002). Radar equations in the problem of radio wave backscattering during bistatic soundings. *Radio Science*, 37(1):8–1–8–8.
- [Berngardt and Kushnarev(2013)] Berngardt, O. I. and Kushnarev, D. S. (2013). Effective subtraction technique at the Irkutsk Incoherent Scatter Radar: Theory and experiment. *Journal of Atmospheric and Solar-Terrestrial Physics*, 105-106:293–298.
- [Berngardt et al.(2015a)] Berngardt, O. I., Kutelev, K. A., Kurkin, V. I., Grkovich, K. V., Yampolsky, Y. M., Kashcheyev, A. S., Kashcheyev, S. B., Galushko, V. G., Grigorieva, S. A., and Kusonsky, O. A. (2015a). Bistatic Sounding of High-Latitude Ionospheric Irregularities Using a Decameter EKB Radar and an UTR-2 Radio Telescope: First Results. *Radiophysics and Quantum Electronics*, 58(6):390–408.
- [Berngardt et al.(2015b)] Berngardt, O. I., Voronov, A. L., and Grkovich, K. V. (2015b). Optimal signals of Golomb ruler class for spectral measurements at EKB SuperDARN radar: Theory and experiment. *Radio Science*, 50(6):486–500. 2014RS005589.
- [Bilitza et al.(2011)] Bilitza, D., Mckinnell, L.-A., Reinisch, B., and Fuller-Rowell, T. (2011). The international reference ionosphere today and in the future. *Journal of Geodesy*, 85(12):909–920.
- [Chisham et al.(2007)] Chisham, G., Lester, M., Milan, S., Freeman, M., Bristow, W., McWilliams, K., Ruohoniemi, J., Yeoman, T., Dyson, P., Greenwald, R., Kikuchi, T., Pinnock, M., Rash, J., Sato, N., Sofko, G., Villain, J.-P., and Walker, A. (2007). A decade of the Super Dual Auroral Radar Network (SuperDARN): scientific achievements, new techniques and future directions. *Surv. Geophys.*, (28):33–109.
- [Farley(1972)] Farley, D. T. (1972). Multiple-pulse incoherent-scatter correlation function measurements. *Radio Science*, 7(6):661–666.
- [Fedoryuk(1989)] Fedoryuk, M. V. (1989). *Analysis I: Integral Representations and Asymptotic Methods*, chapter Asymptotic Methods in Analysis, pages 83–191. Springer Berlin Heidelberg, Berlin, Heidelberg.
- [Gauld et al.(2002)] Gauld, J. K., Yeoman, T., Davies, J. A., Milan, S., and Honary, F. (2002). SuperDARN radar HF propagation and absorption response to the substorm expansion phase. *Annales Geophysicae*, 20:1631–1645.
- [Gillies et al.(2009)] Gillies, R., Hussey, G., Sofko, G., McWilliams, K., Fiori, R. A. D., Ponomarenko, P., and St-Maurice, J.-P. (2009). Improvement of SuperDARN velocity measurements by estimating the index of refraction in the scattering region using interferometry. *Journal of Geophysical Research: Space Physics*, 114(A7):A07305.
- [Gillies et al.(2011)] Gillies, R., Hussey, G., Sofko, G., Ponomarenko, P., and McWilliams, K. (2011). Improvement of HF coherent radar line-of-sight velocities

- by estimating the refractive index in the scattering volume using radar frequency shifting. *Journal of Geophysical Research*, 116:1302.
- [Ginzburg(1970)] Ginzburg, V. L. (1970). *The propagation of electromagnetic waves in plasmas*. Oxford: Pergamon.
- [Greenwald et al.(1995)] Greenwald, R., Baker, K. B., Dudeney, J. R., Pinnock, M., Jones, T., Thomas, E., Villain, J.-P., Cerisier, J. C., Senior, C., Hanuise, C., Hunsucker, R. D., Sofko, G., Koehler, J., Nielsen, E., Pellinen, R., Walker, A., Sato, N., and Yamagishi, H. (1995). Darn/Superdarn: A Global View of the Dynamics of High-Latitude Convection. *Space Science Reviews*, 71:761–796.
- [Heading(1962)] Heading, J. (1962). *An Introduction to Phase-Integral Methods*. John Wiley, London.
- [Ishimaru(1978)] Ishimaru, A. (1978). *Wave Propagation and Scattering in Random Media*. Academic Press, New York.
- [Kravtsov and Namazov(1980)] Kravtsov, Yu. A. and Namazov, S. A. (1980). Characteristics of scattering of radio waves from magnetically oriented inhomogeneities of the ionosphere near critical frequency (in russian). *Radiotekhnika i Elektronika*, 25:459–466.
- [Kravtsov and Orlov(1990)] Kravtsov, Yu. A. and Orlov, Yu. I. (1990). *Geometrical Optics of Inhomogeneous Media*. Springer Series on Wave Phenomena. Springer-Verlag Berlin Heidelberg.
- [Kravtsov et al.(1996)] Kravtsov, Yu. A., Naida, O. N., and Fuki, A. A. (1996). Waves in weakly anisotropic 3D inhomogeneous media: quasi-isotropic approximation of geometrical optics. *Physics-Uspekhi*, 39 2:129–154.
- [Lataitis(1992)] Lataitis, R. (1992). Signal power for radio acoustic sounding of temperature: The effects of horizontal winds, turbulence, and vertical temperature gradients. *Radio Science*, 27(3):369–385.
- [Lehtinen(1986)] Lehtinen, M.S. (1986). Statistical theory of incoherent scatter radar measurements *Ph.D.Thesis*, , University of Helsinki, Helsinki
- [Liang and Wan(1997)] Liang, J. and Wan, W. (1997). HF propagation and scattering in a turbulent ionosphere with an anisotropic and inhomogeneous background. *Radio Science*, 32(3):1011–1021.
- [Nasyrov(1991)] Nasyrov, A. M. (1991). *Scattering of radiowaves from anisotropic ionospheric irregularities (in russian)*. Kazan University.
- [Ponomarenko et al.(2009)] Ponomarenko, P., St-Maurice, J.-P., Waters, C. L., Gillies, R., and Koustov, A. (2009). Refractive index effects on the scatter volume location and Doppler velocity estimates of ionospheric HF backscatter echoes. *Annales Geophysicae*, 27:4207–4219.
- [Ponomarenko et al.(2010)] Ponomarenko, P., St-Maurice, J.-P., Hussey, G., and Koustov, A. (2010). HF ground scatter from the polar cap: Ionospheric propagation and ground surface effects. *Journal of Geophysical Research: Space Physics*, 115:10310.
- [Ponomarenko et al.(2011)] Ponomarenko, P., Koustov, A., St-Maurice, J.-P., and Wiid, J. (2011). Monitoring the F-region peak electron density using HF backscatter interferometry. *Geophysical Research Letters*, 38(21):DOI:10.1029/2011gl049675.
- [Ribeiro et al.(2013)] Ribeiro, A. J., Ponomarenko, P., Ruohoniemi, J., Baker, J., N. Clausen, L. B., Greenwald, R., and de Larquier, S. (2013). A realistic radar data simulator for the Super Dual Auroral Radar Network. *Radio Science*, 48(3):283–288.
- [Ruohoniemi et al.(1988)] Ruohoniemi, J., Greenwald, R., Villain, J.-P., Baker, K. B., Newell, P. T., and Meng, C. I. (1988). Coherent HF radar backscatter

- from small-scale irregularities in the dusk sector of the subauroral ionosphere. *Journal of Geophysical Research: Space Physics*, 93(A11):12871–12882.
- [Ruohoniemi et al.(1989)] Ruohoniemi, J., Greenwald, R., Baker, K. B., Villain, J.-P., Hanuise, C., and Kelly, J. (1989). Mapping high-latitude plasma convection with coherent HF radars. *Journal of Geophysical Research: Space Physics*, 94(A10):13463–13477.
- [Ruohoniemi et al.(2011)] Ruohoniemi, J., Greenwald, R., Ribeiro, A. J., Clausen, L. B. N., Baker, J., Frissell, N., and K.A., S. (2011). SuperDARN ionospheric space weather. *Aerospace and Electronic Systems Magazine, IEEE*, pages 30–34.
- [Schiffler(1996)] Schiffler A.(1996), SuperDARN measurements of double-peaked velocity spectra. *M.Sc. Thesis*, University of Saskatchewan, Saskatoon
- [Settimi et al.(2014)] Settimi, A., Ippolito, A., Cesaroni, C., and Scotto, C. (2014). Scientific review on the ionospheric absorption and research prospects of a complex eikonal model for one-layer ionosphere. *International Journal of Geophysics*, 2014.
- [Settimi et al.(2015)] Settimi, A., Pietrella, M., Pezzopane, M., and Bianchi, C. (2015). The IONORT-ISP-WC system: Inclusion of an electron collision frequency model for the D-layer. *Advances in Space Research*, 55(8):2114 – 2123.
- [Spaleta et al.(2015)] Spaleta, J., Bristow, W., and Klein, J. (2015). Temporal and spatial resolved SuperDARN line of sight velocity measurements corrected for plasma index of refraction using Bayesian inference. *Journal of Geophysical Research*, 120:3207–3225.
- [Tatarsky(1967)] Tatarsky, V. I. (1967). *Wave Propagation in a Turbulent Atmosphere (in russian)*. Nauka, Moscow.
- [Uspensky et al.(1994a)] Uspensky, M., Koustov, A., Sofko, G., Koehler, J. A., Villain, J.-P., Hanuise, C., Ruohoniemi, J., and Williams, P. J. S. (1994a). Ionospheric refraction effects in slant range profiles of auroral HF coherent echoes. *Radio Science*, 29(2):503–517.
- [Uspensky et al.(1994b)] Uspensky, M. V., Williams, P. J. S., Romanov, V. I., Pivovarov, V. G., Sofko, G. J., and Koehler, J. A. (1994b). Auroral radar backscatter at off-perpendicular aspect angles due to enhanced ionospheric refraction. *Journal of Geophysical Research: Space Physics*, 99(A9):17503–17509.

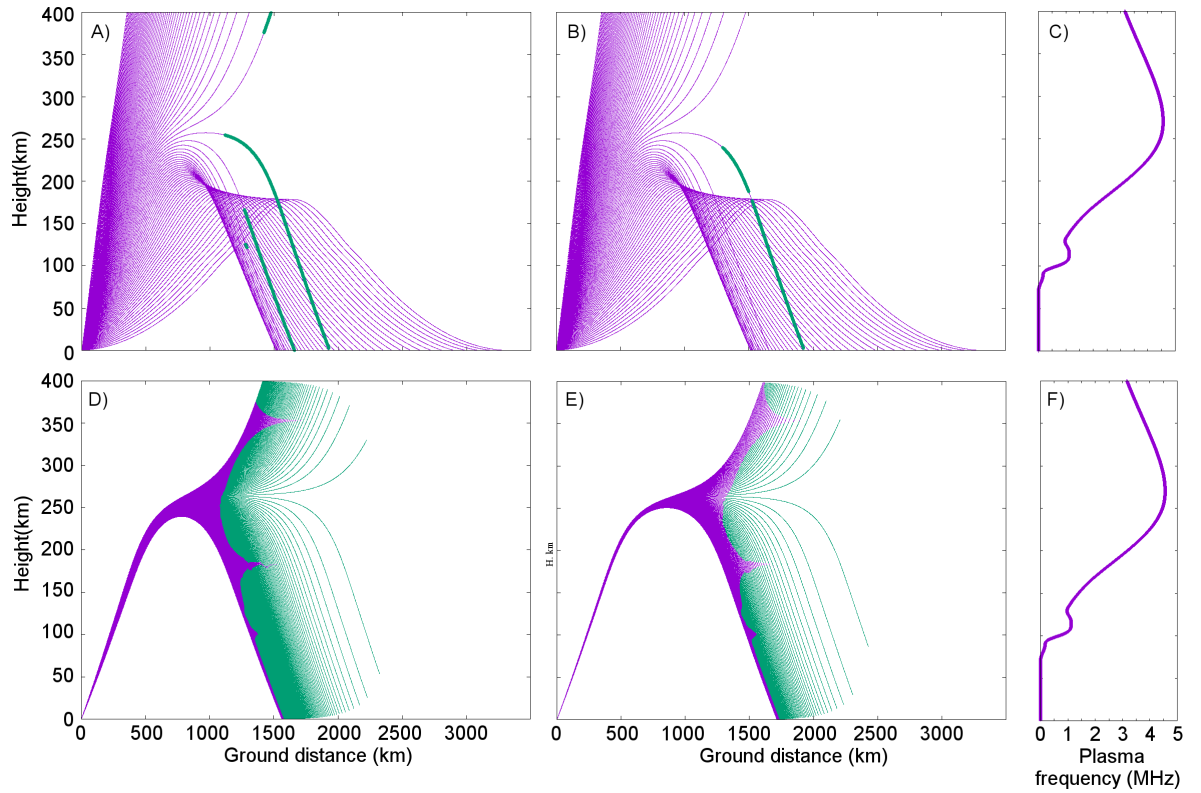


FIGURE 1. Regions of narrowband approximation validity (A,B,D,E) and ionospheric profile (C,F) used for modeling. Blue color corresponds to the validity region for initial equations (11). Pulse duration is A,D) - 100 usec; B,E) - 300usec. A,B) - wide exit ray angles range, D,E) - only trajectories near Pedersen ray.

INSTITUTE OF SOLAR-TERRESTRIAL PHYSICS SB RAS, 664033, 126A, LERMONTOVA STR., IRKUTSK, RUSSIA, P.O.BOX 291, E-MAIL: BERNG@ISZF.IRK.RU

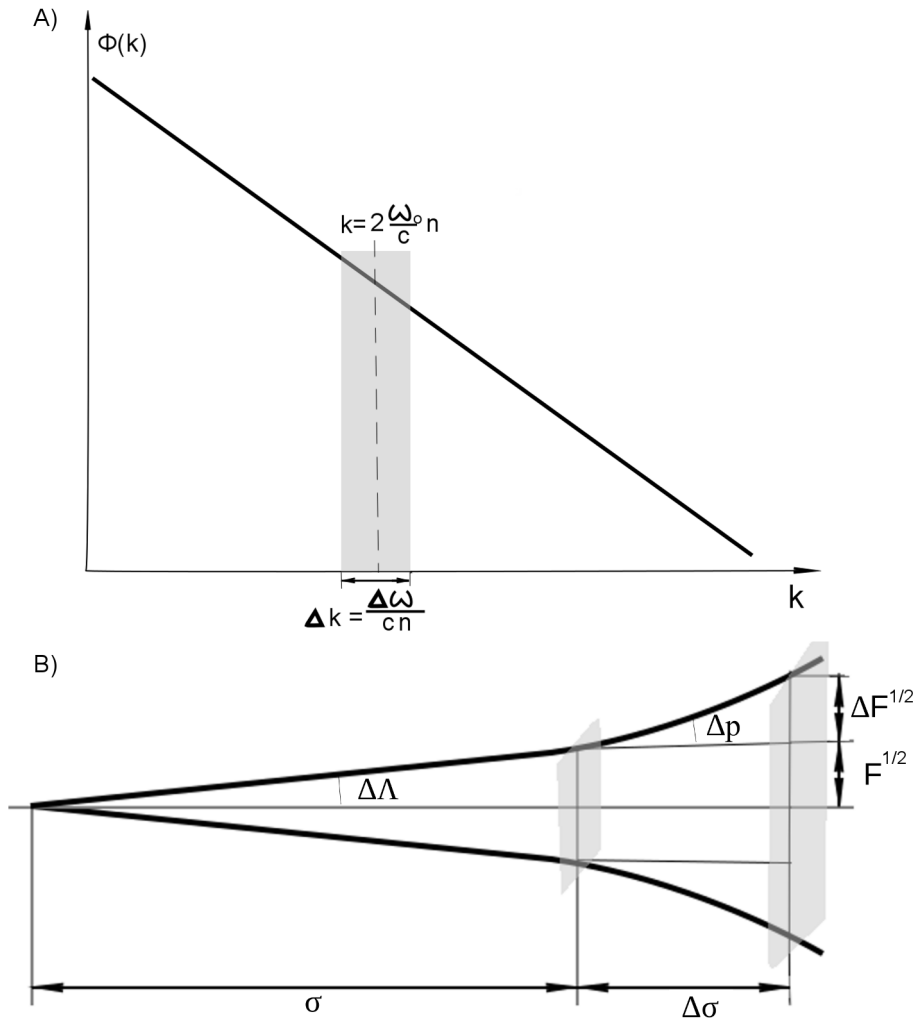


FIGURE 2. A) Selective properties of scattering for the locally-homogeneous monostatic case (40,43). B) Geometrical considerations for calculating  $J_{\hat{P} \rightarrow \hat{\Lambda}}$

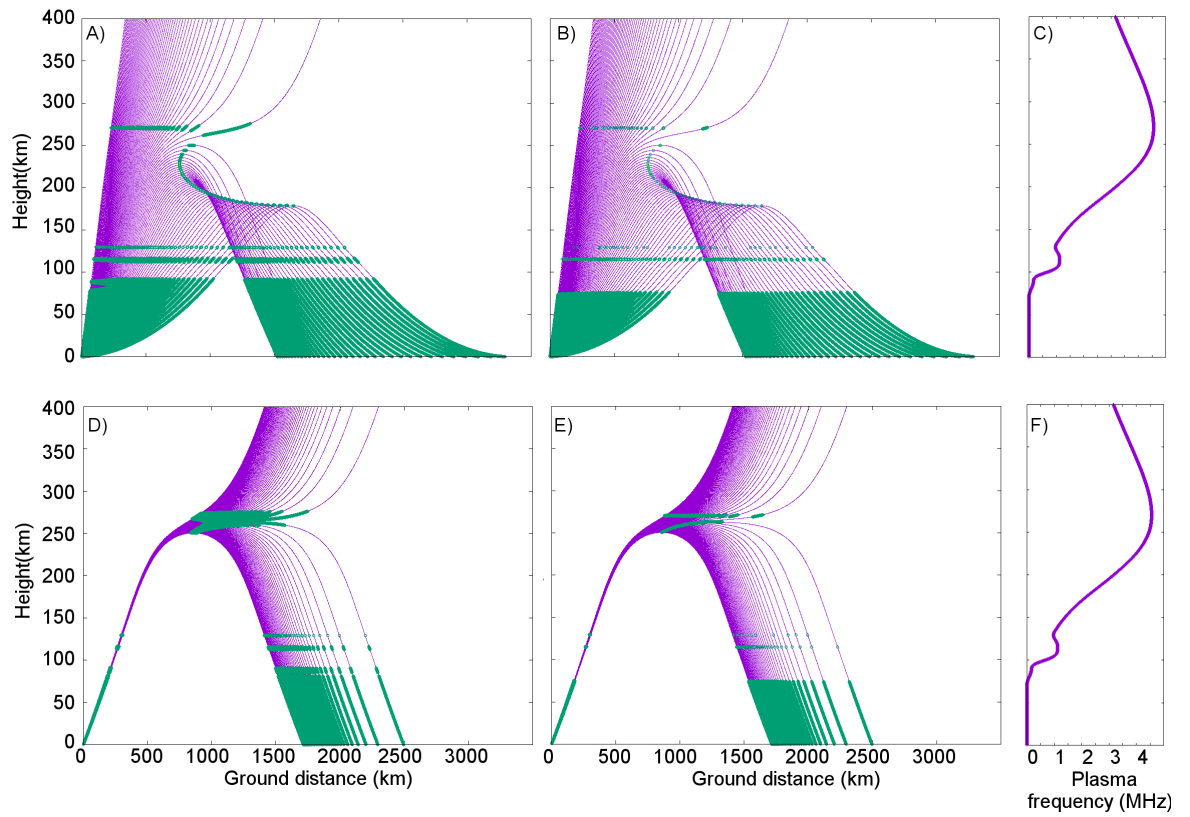


FIGURE 3. The areas of locally-homogeneous trajectories in the ionosphere. Green areas corresponds to locally-homogeneous cases. A,D) for 100usec sounding pulse, B,E) for 300usec sounding pulse, C,F) plasma frequency profile used in the calculations. D-E) - the detailed areas near the Pedersen ray.

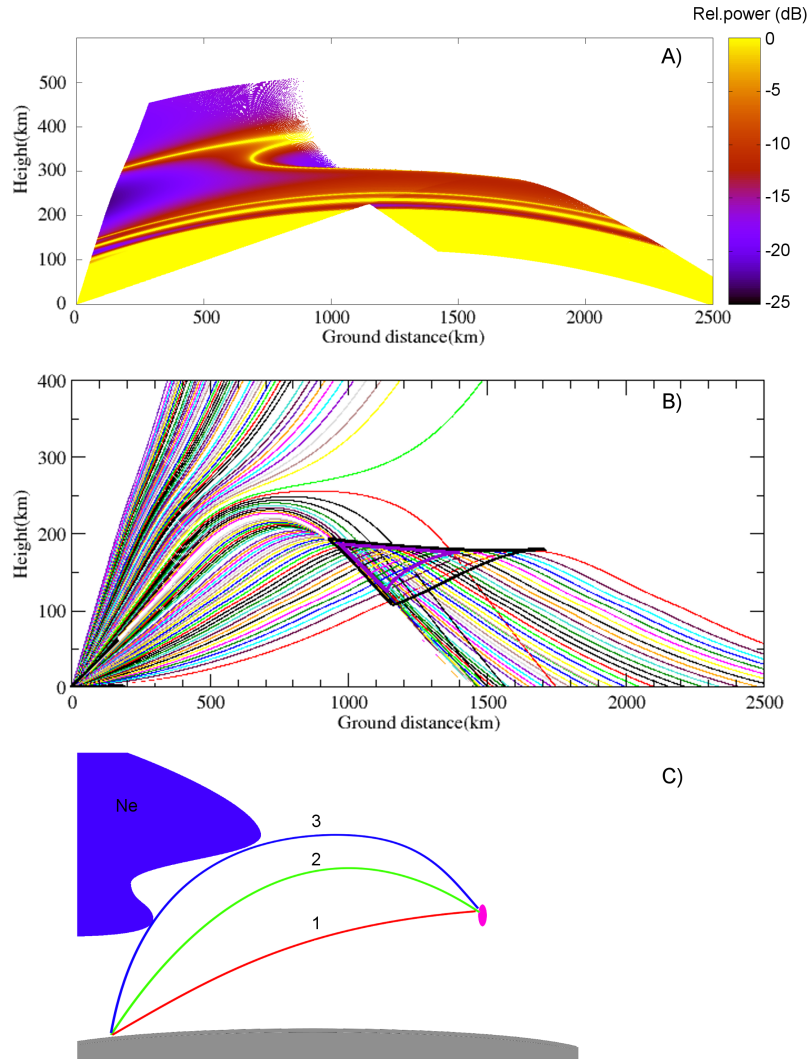


FIGURE 4. Propagation effects in the radar equation. A) Effect of refraction to the scattered signal power ( $(J_1/\Delta R_A)^2$  relation). Yellow areas corresponds to the scattering at locally-homogeneous trajectories, red and blue - at locally-inhomogeneous trajectories. B) The trajectories of the ray propagation. Multiple trajectory case region is marked with a black triangle. Region with 3 trajectories to any scattering point is marked with blue triangle. C) The geometry of the multiple trajectory sounding.

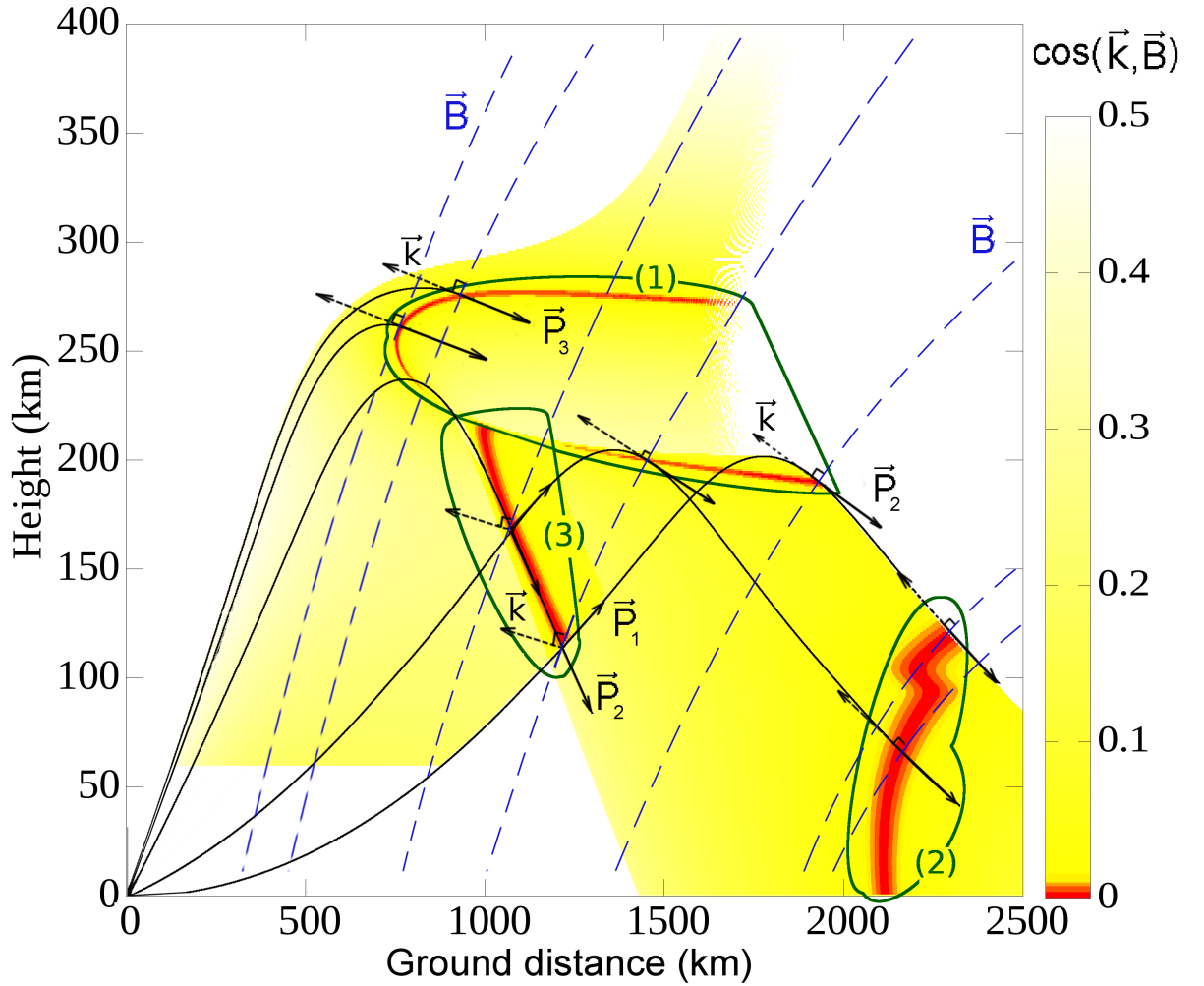


FIGURE 5. Model calculations for regions of most intensive scattering from field-aligned irregularities for a radar, located at north magnetic pole and looking to the equator (calculations are based on IGRF reference magnetic field model and IRI-2012 reference ionosphere model). Black lines - ray trajectories  $R(\hat{\Lambda}, S)$ ; blue lines - magnetic field  $\vec{B}$  lines ; green regions - orthogonality regions for monostatic scattering at F-layer heights (1), for monostatic scattering at E-layer heights (2) and for multi-trajectory scattering (3).